PALÆO
VERTEBRATA

Morphological description and identification of an extraordinary new elephant cranium from the early Pliocene of Ileret, Kenya

William J. SANDERS[a, b*], **Meave G. LEAKEY**[c], **Louise N. LEAKEY**[c], **Craig S. FEIBEL**[d, e], **Timothy Gichunge IBUI**[f, g], **Cyprian NYETE**[h], **Mbatha Pauline MBETE**[g], **Francis H. BROWN**[†i]

[a]*Museum of Paleontology, University of Michigan, 1105 North University Avenue, Ann Arbor, Michigan 48109, United States*
[b]*Department of Anthropology, University of Michigan, 1085 South University Avenue, Ann Arbor, Michigan 48109, United States*
[c]*Turkana Basin Institute, Stony Brook University, Circle Road, SBS Building S-501, Stony Brook, New York, 11794, United States*
[d]*Department of Earth and Planetary Sciences, Rutgers University, 610 Taylor Road, Piscataway, New Jersey 08854, United States*
[e]*Department of Anthropology, Rutgers University, 131 George Street, New Brunswick, New Jersey 08901, United States*
[f]*Turkana Basin Institute, Hardy Post 2nd Floor, Ushirika Road, Karen P.O. Box 24467, Nairobi 00502, Kenya*
[g]*National Museums of Kenya, Museum Hill, P.O. Box 40658, Nairobi 00100, Kenya*
[h]*Turkana Basin Institute, Ileret, Kenya, c/o P.O. Box 24467, Nairobi 00502, Kenya*
[i]*Department of Geology and Geophysics, University of Utah, 115 S 1460 E, Salt Lake City 84112, United States*

**corresponding author: wsanders@umich.edu*
†Francis H. Brown is deceased and this paper is dedicated to his memory

Abstract: Paleontological exploration in the Turkana Basin near Ileret, Kenya yielded the most complete adult elephant cranium (KNM-ER 63642) known from the late Miocene to mid-Pliocene. KNM-ER 63642 derives from the lower Lonyumun Mb. of the Koobi Fora Fm. and dates to the early Pliocene, >4.3 Ma. The cranium is immense in size and preserves most of its structures including left and right M2-3, permitting its comprehensive comparative study and secure taxonomic assignment to *Loxodonta adaurora*. Features distinctive of the species and exhibited by KNM-ER 63642 include very elongate, divergent tusk alveoli, a short, biconvex cranial roof, anterosuperior angulation of the occipital planum, non-inflated occipital planum and absence of supralateral parietal "bossing," broad, flat premaxillary nasal processes, broad, laterally downturned nasal aperture superior to the level of the orbits, and M3s with wide, subhypsodont plates that are parallel-faced and separated by U-shaped transverse valleys. The M3s also exhibit characteristic *L. adaurora* traits of greatest width at their bases, rounded cross-sectional shape, thick enamel, abundant cementum, and strong anterior and posterior accessory conules. Of extant taxa, KNM-ER 63642 most closely resembles crania of African elephants. Its inclusion in the *Loxodonta* clade is tenuous, however, because shared features are either symplesiomorphic or are difficult to test for synapomorphy due to the poor fossil record of crania of late Miocene-early Pliocene elephants. Overall, the cranial morphology of KNM-ER 63642 is unexpectedly advanced for an elephant of its antiquity. Its anteroposterior compression and height are concordant with efficient proal masticatory action, indicating that by the early Pliocene *L. adaurora* evolved craniodental adaptations in phase with feeding preference for C_4 grasses. The advantage of synchrony of morphology and behavior is reflected by the dominance of the species in the greater Turkana Basin during that interval.

Keywords: Elephantidae, *Loxodonta adaurora*, cranium, early Pliocene, Ileret, Kenya

Submitted 23 April 2021, Accepted 13 July 2021

INTRODUCTION

Paleontological exploration of sedimentary outcrops at Area 14 near Ileret, Kenya (Figure 1) in 2013 led to the recovery of an immense fossil elephant cranium preserving left and right M2-3s (field number F26411). The cranium was discovered by Mr. Apollo Longaye, a member of the Koobi Fora Research Project. Only a single molar was visible at the surface when the specimen was discovered (Figure 2A), and no other fossils were found in association. Excavation revealed the presence of a nearly complete cranium, (Figure 2B), which was chemically treated in situ with an archival consolidant because of its fragile condition. It was then cradled in a plaster jacket secured to a steel frame. The cranium was hoisted from its field location using a block-and-tackle suspended from a large metal scaffold into a vehicle for transport to the Ileret Facility of the Turkana Basin Institute (Figure 2C, D). Weight of the cranium and surrounding matrix in the plaster jacket and metal frame was estimated during this process to be approximately two tons. It underwent careful preparation (see Figure 2E, F) and additional chemical consolidation in stages, and is now permanently accessioned at the facility as KNM-ER 63642.

The new elephant cranium derives from the Lonyumun Mb. of the Koobi Fora Fm. (Fig. 3A; Brown & Feibel, 1986; Brown & McDougall, 2011). This geological unit is characterized by claystones with one or more prominent diatomites, heavily altered to clay minerals and opal CT, representing the fine-grained lacustrine sequence of the Lonyumun Lake. In the Ileret region, Gathogo & Brown (2006) recognized three lithofacies intervals comprising the Lonyumun: A lower sequence of predominantly sandstones and conglomerates reflecting fluvial deposition, a second sequence consisting of claystones, diatomites and ostracod sandstones deposited in a lacustrine setting, and a third, upper interval including upward-coarsening silt and sandstone units indicative of a deltaic setting. Farther north, Kidney (2012) documented correlative

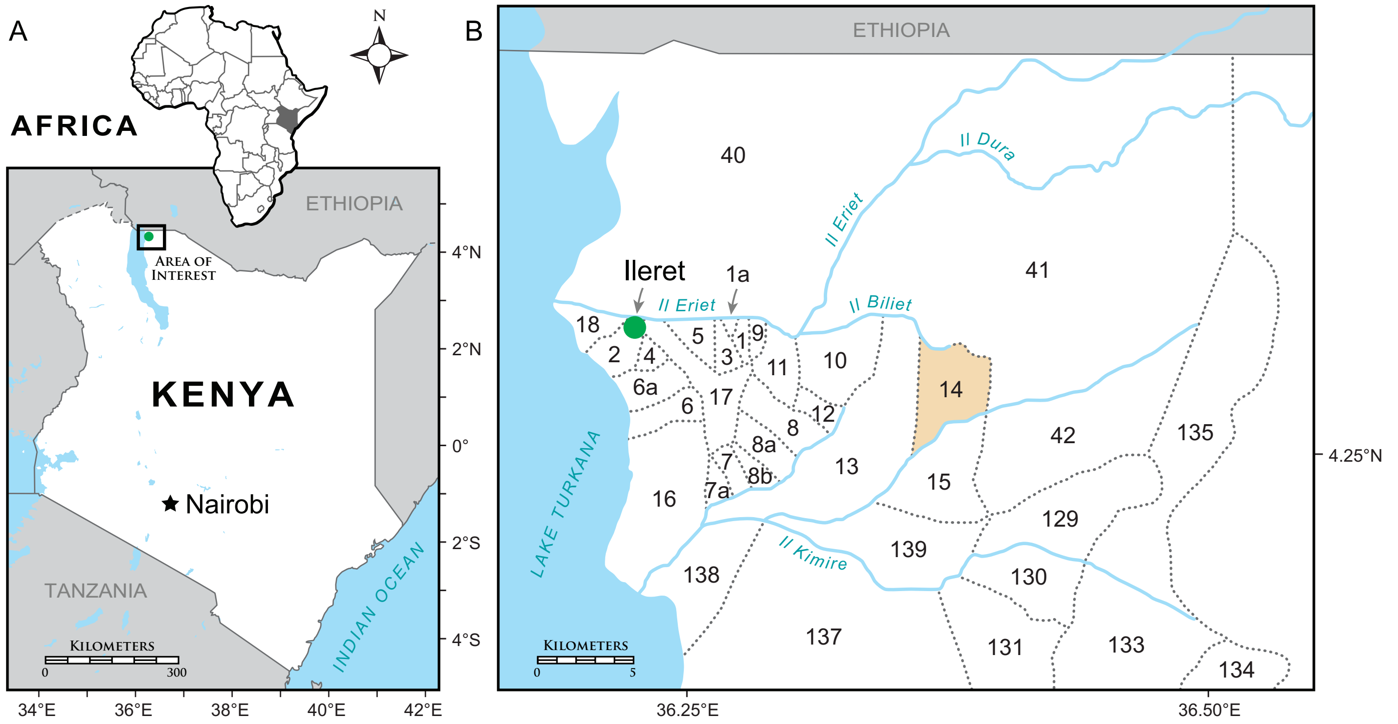

Figure 1. Maps showing the geographic position of Ileret, Kenya and locality Area 14. **A**, Map of the area of interest for the recovery of elephant cranium KNM-ER 63642 (*Loxodonta adaurora*), the Ileret Region at the northeast side of Lake Turkana. The green dot indicates the position of Ileret. **B**, Detailed map of localities in the area of interest (Ileret Region). KNM-ER 63642 was recovered from Area 14 (highlighted).

lacustrine and deltaic intervals, with four tephra within the upper interval all capped by the Moiti Tuff.

In Area 14, the local sequence associated with the elephant cranium consists of a prominent quartzo-feldspathic sand with large-scale trough cross bedding, lying 3–5 m below the lowest prominent diatomite of the fine-grained interval (Figure 3B). The cranium was excavated from the sandstone. At this locality, outcrops are relatively subdued and rounded by erosion, but excellent high-relief outcrops just 1.5 km to the northeast display the same characteristic sequence, in which the lighter-colored lower fluvial interval is dominated by the major channel sandstone, and the sharp transition to dark fine-grained strata marks the transition to the lacustrine interval (Fig. 3C).

Kidney (2012) established a potential age range of 4.49–4.29 Ma for the diatomites of the Lonyumun Mb. based upon his magnestostratigraphic analysis placing the lacustrine interval of Gathogo's (2003) section 41-2 entirely within Chron C3N1r, the reversed polarity magnetozone below the Cochiti Subchron. The stratigraphic position of the sand body from which the elephant fossil was recovered 3 m below the lower diatomite suggests a datation of >4.3 Ma (and possibly >4.5 Ma) for this fossil. This age is broadly comparable to the Apak Mb. of the Nachukui Fm. at Lothagam, Kenya (Feibel, 2003; McDougall & Feibel, 1999), and is slightly older than the Kanapoi Fm. at Kanapoi, Kenya (Feibel, 2003; McDougall & Brown, 2008; Brown & McDougall, 2011; Sanders, 2020).

The age of KNM-ER 63642 places the specimen in an early Pliocene "relay" interval of elephant evolution, during which archaic elephant species and basal members of crown elephant lineages that first appeared in the late Miocene-earliest Pliocene, such as *Stegotetrabelodon orbus*, *Stegodibelodon schneideri*, *Selenetherium kolleensis*, *Primelephas korotorensis*, *Mammuthus subplanifrons*, and *Loxodonta cookei*, were replaced or succeeded by more advanced species including *Loxodonta adaurora*, *L. exoptata*, "*Elephas*" *ekorensis*, *E. recki*, and a more derived form of *Mammuthus*, *M.* sp. "Hadar-type," morphologically intermediate dentally between late Miocene-earliest Pliocene *M. subplanifrons* and mid-to-late Pliocene *M. africanavus* (Coppens, 1965, 1972; Arambourg, 1970; Maglio, 1970, 1973; Maglio & Hendey, 1970; Maglio & Ricca, 1977; Coppens *et al.*, 1978; Beden, 1983, 1987a, b; Mebrate, 1983; Hill *et al.*, 1985; Kalb & Mebrate, 1993; Sanders, 1997, 2007, 2008, 2011, 2020, in press; Tassy, 1995, 2003; Mackaye, 2001; Mackaye *et al.*, 2005, 2008; Saegusa & Haile-Selassie, 2009; Sanders *et al.*, 2010; Sanders & Haile-Selassie, 2012).

The late Miocene-early Pliocene also comprised a phase during which diverse gomphotheriid lineages began to disappear from Africa, stressed by ecological change and competition with elephants that had evolved substantial morphological innovations, presumably providing them life history advantages and more effective masticatory adaptations to new resources (Sanders *et al.*, 2010). Elephants have block-like molars formed of lamellae, or plates, held together by cementum (Roth, 1989; Lister, 2013), which are efficiently driven by muscles deployed around foreshortened mandibles and anteroposteriorly compressed, raised crania (Maglio, 1972, 1973) in proal masticatory function, or fore-aft horizontal shearing (Saegusa, 2020). Within Proboscidea, elephant molars are highly derived and their evolution involved transformation from gomphotheriid-type molars comprised of cusps, conelets, and conules arranged in complementary half-loph(id)s. The ontogenetic development of elephant molars is complex and involves configuration of dental epithelium into deep folds that become lamellae separated by transverse valleys, growth of enamel surrounding the dentine and pulp cavities of the lamellae, from the apex downward, thickening and union of

Figure 2. Recovery stages of elephant cranium KNM-ER 63642 (*Loxodonta adaurora*) from Area 14, near Ileret, Kenya. **A**, Right M3 of the cranium, visible on surface. **B**, Excavation of the cranium, ventral side up in situ. **C**, **D**, Block-and-tackle lifting cranium in its plaster jacket, secured on a metal frame, and placement in the vehicle for transport. **E**, **F**, Anterior and right lateral views of the cranium following initial manual and mechanical preparation at the Ileret Turkana Basin Facility. Length from the nuchal crest to the distal end of the incisor alveoli measures 1367 mm, and greatest width across the orbits is 837 mm.

lamellae that are further infilled with dentine, and consolidation of lamellae by an external covering of cementum (Roth, 1989).

It was hypothesized that the formation of molar plates and transformation of skull anatomy to drive fore-aft horizontal masticatory shearing evolved in elephants as adaptive responses to grazing (Maglio, 1972, 1973). Apically worn plate surfaces comprise a series of enamel blades orthogonal to the direction of mastication that are highly efficient shearing surfaces for maximum use of the occlusal surface, that are very effective at slicing grasses (Maglio, 1972; Koenigswald, 2016; Saegusa, 2020). Indeed, dental isotopic evidence demonstrates that some populations of early elephants incorporated substantial amounts of C_4 grasses in their diets (Cerling *et al.*, 1999, 2003a, b; Kingston, 1999; Uno *et al.*, 2011), concomitant with climatic and environmental changes in the late Miocene that favored the spread of partially open grassy woodlands and

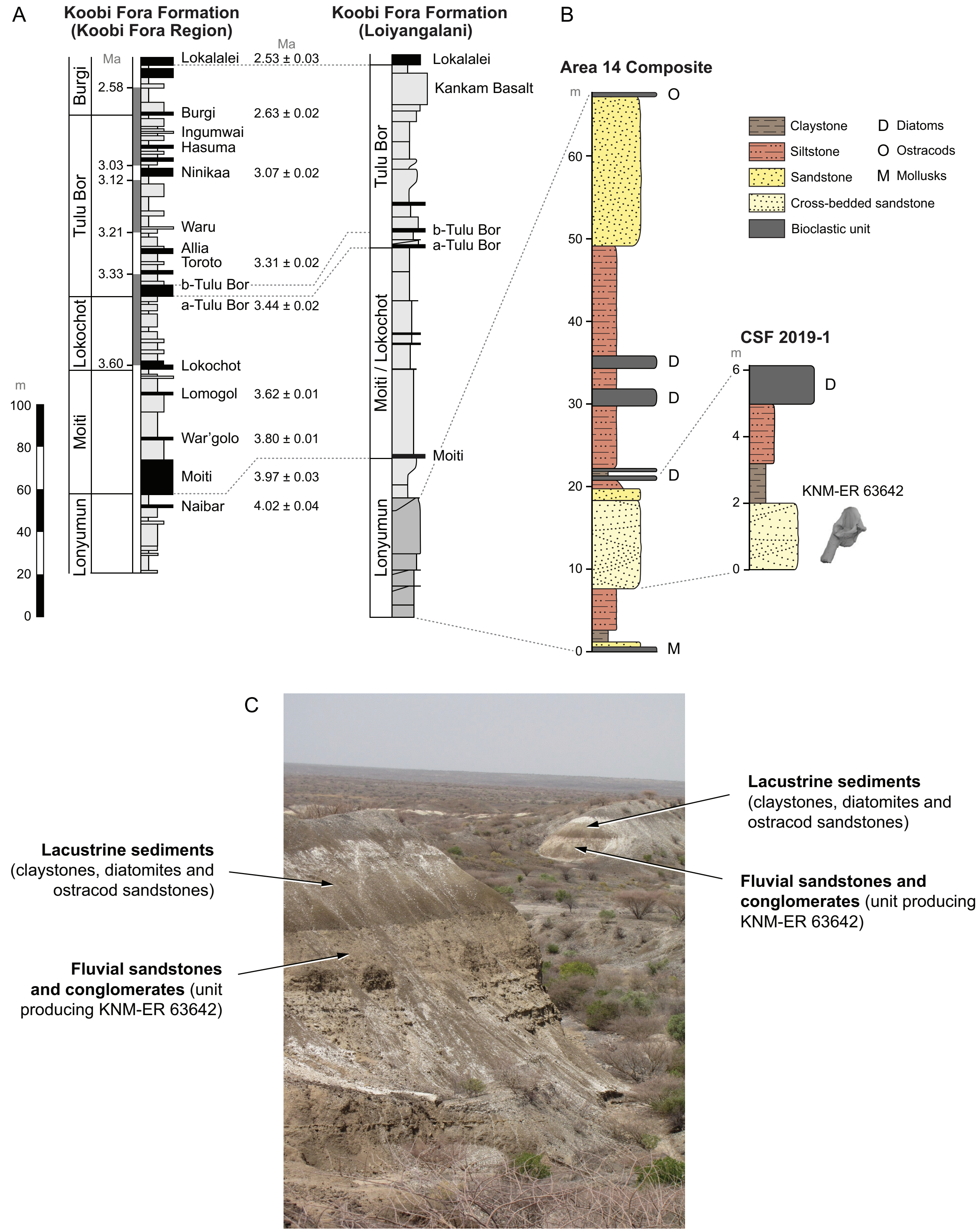

Figure 3. Stratigraphic provenience of KNM-ER 63642 in the lower Lonyumun Member of the Koobi Fora Formation at Area 14, Ileret, Kenya. **A**, Chronostratigraphy of the Koobi Fora Formation, showing the position of the Lonyumun Member, modified from Brown & McDougall (2011). **B**, Composite stratigraphic section of the lower Lonyumun Member in Area 14, and stratigraphic section of the lower Lonyumun Member at the elephant cranium (KNM-ER 63642) excavation locality, based on field observations of CSF. **C**, Outcrops of the lower Lonyumun Member of the Koobi Fora Formation, located 1.5 km northeast of the KNM-ER 63642 (*Loxodonta adaurora*) locality in Area 14. KNM-ER 63642 was excavated from the fluvial sand interval.

savannas (Cerling *et al.*, 1997; Strömberg, 2011), including in the region around Lake Turkana (Fortelius *et al.*, 2016, Saarinen, 2019). Conversely, limited isotopic sampling of teeth of stegotetrabelodonts and *Primelephas korotorensis* from the late Miocene Lukeino Fm., Tugen Hills, Kenya produced evidence that in that area they were either dedicated browsers or mixed-feeders (Roche *et al.*, 2013; Doman, 2017).

Though consistent with instances of browsing, however, the morphology of late Miocene-earliest Pliocene elephant molars suggests that in populations that were exploiting C_4 grasses, feeding behavior was out of phase with, and preceded, advanced gnathodental adaptations for grazing (Lister, 2013). The molars of these primitive elephants have few, widely-spaced plates, very thick, unfolded enamel, modest coatings of crown cementum, pyramidal, bulbous lateral plate profiles, and are very low-crowned (brachyodont). Presumably, with the increasing spread of wooded savannas and associated C_4 resources through the Pliocene in East Africa (Cerling *et al.*, 2011 a, b; Levin *et al.*, 2011), coupled with larger numbers of mammalian taxa competing for these resources (including anancine gomphotheres, stegodonts, and multiple elephant species) (Cerling *et al.*, 1999; 2011a; Zazzo *et al.*, 2000; Leakey & Harris, 2003; Kingston & Harrison, 2007; Levin *et al.*, 2008, 2011; Sanders *et al.*, 2010; Kingston, 2011; Uno *et al.*, 2011; Manthi *et al.*, 2017), selective pressures ratcheted up for greater effectiveness at grazing, favoring Pliocene successor or replacement elephant species with higher-crowned molars constructed of a greater number of plates and with a thicker covering of cementum that were more durable against dental attrition from chewing grit incorporated in food acquired low to the ground and opal phytoliths in C_4 grasses (Lister, 2013; Sanders, 2020). However, it is less well known if elephant crania underwent accompanying changes to improve muscular action for proal movement of lower against upper jaws and teeth.

KNM-ER 63642 is extraordinary because it preserves a wealth of anatomical detail and is the most complete elephant cranium known from the inception of elephants in the late Miocene until nearly the mid-Pliocene, an interval that constitutes more than half of the existence of the Elephantidae. Crania of stegotetrabelodonts (Petrocchi, 1943, 1954; Tassy, 1999, 2003; Sanders, in press), *P. korotorensis* (Tassy, 1995), *L. adaurora* (Maglio, 1970, 1973; Maglio & Ricca, 1977; Beden, 1983, 1987a; Sanders, 2020), and "*E.*" *ekorensis* (Maglio, 1970, 1973; Maglio & Ricca, 1977) were previously recovered from fossil beds within this interval. These few specimens, however, are frustratingly incomplete and heavily damaged, limiting their utility for testing Lister's (2013) hypothesis about asynchrony of feeding behavior and cranio-masticatory adaptations in early elephants. The new Ileret cranium provides an opportunity to robustly assess the correlative link between craniodental evolution and feeding behavior in early elephants during their early Pliocene "relay" interval.

Morphological and metric comparison of KNM-ER 63642 with craniodental remains of late Miocene and early Pliocene elephants, restricted during this interval to Afro-Arabia, definitively show that its closest similarity is with partial crania of early Pliocene *Loxodonta adaurora*. This species was first recognized by Maglio (1970), who distinguished it from more primitive, late Miocene-early Pliocene *Stegotetrabelodon orbus* and *Primelephas korotorensis* (then *P.* "*gomphotheroides*") and more derived, contemporaneous "*Elephas" ekorensis*, which were all named in the same publication. *Loxodonta adaurora* is an eastern African species best known from sites proximal to the greater Turkana Basin. It is well documented dentally and by most elements of its skeleton (Maglio, 1970, 1973; Maglio & Ricca, 1977; Beden, 1983, 1987a; Harris *et al.*, 1988, 2003; Sanders, 2020). Chronostratigraphic provenience of KNM-ER 63642 in the lower Lonyumun Member of the Koobi Fora Formation indicates that it is among the oldest securely dated specimens of *L. adaurora*.

Although the molars of *L. adaurora* lack the development of well-formed loxodont sinuses ("<>") that characterize molars of the extant African elephants, *L. africana* and *L. cyclotis*, and to varying degrees the fossil species *L. cookei*, *L. exoptata*, and *L. atlantica* (Maglio, 1973; Sanders, 2007, 2011; Sanders *et al.*, 2010) in their enamel wear figures, despite the presence of strong anterior and posterior accessory conules, the closer resemblance of cranial and postcranial remains of the fossil species to African elephants, rather than mammoths or Asian elephants, led Maglio (1970) to place it in *Loxodonta*. Despite exhibiting a cranial configuration typical of some geologically younger elephant species ("acrocephalic," or raised and anteroposteriorly truncated), nothing in the morphology of partial crania of *L. adaurora* or KNM-ER 63642 is synapomorphic with derived features that individually define the crania of *Mammuthus*, *Elephas*, or *Palaeoloxodon*, such as parietal bossing, inflation of the nuchal planum, development of a parieto-occipital crest, hypertrophy of the occipital over the apex of the vault, or frontal concavity (see Maglio, 1973; Lister *et al.*, 2005; Todd, 2006; Sanders *et al.*, 2010; Zhang *et al.*, 2018; Larramendi *et al.*, 2020). Nonetheless, there is no question that *L. adaurora* is a well-delineated species (Sanders, 2020). Confirmation of Maglio's (1970) generic assignment, however, relies in part on whether cranial morphological features shared by *L. adaurora* and extant African elephants are synapomorphic, or symplesiomorphic.

In a number of aspects, KNM-ER 63642 is morphologically advanced. The completeness of the specimen permits unequivocal confirmation that in *L. adaurora* the cranium is considerably more raised and markedly more anteroposteriorly compressed than in middle Miocene gomphotheres (Tassy, 2013) and is generally similar to other elephants in this regard. Consequences of this evolutionary reorganization of the cranium include retraction of molars posterior to the position of the orbit, narrowing of the temporal fossa and more vertical orientation of the temporalis muscle, a higher basicranium and deeper molar alveolus, stronger downturn of the rostrum, and a taller occipital planum angled forward superiorly. These differences are accompanied in *L. adaurora* by loss of lower tusks and a relatively much shorter symphysis and deeper mandibular corpus (Sanders, 2020), compared with the condition in gomphotheres (Tassy, 2013) and some of the mandibular features of the most primitive elephants (Petrocchi, 1954; Maglio, 1970, 1973; Maglio & Ricca, 1977; Kalb & Mebrate, 1993; Tassy, 1999; Mackaye *et al.*, 2005, 2008; Saegusa & Haile-Selassie, 2009; Sanders, in press). As a result, in *L. adaurora* higher-crowned molars could develop in their crypts, the center of mass of the lower jaw was more posteriorly located, and the temporalis muscle was more vertically oriented. In this context, KNM-ER 63642 provides powerful additional evidence to test the hypothesis that by the early Pliocene at least one elephant lineage possessed craniodental adaptations that corresponded more closely with feeding behavior (Lister, 2013).

Geological abbreviations

Fm., geological formation; **Mb.**, geological member; **Ma**, mega annum (million years).

Morphological and dimensional abbreviations

dP/dp, upper or lower deciduous premolar, for example dp4 is a lower fourth deciduous premolar; **ET**, enamel thickness; **H**, height; **HI**, hypsodonty index, H/W x 100; **l.**, left; **L**, length; **LF**, lamellar frequency, number of loph(id)s or plates per 100 mm; **M**, upper molar, for example M2 is an upper second molar; **mm**, millimeter; **mp**, megapixel; **P**, upper premolar, for example P3 is an upper third premolar; **r.**, right; **W**, width; **x**, anterior or posterior cingulum(id); **X**, large anterior or posterior cingulum(id) forming an incipient loph(id) or plate; **+**, indicates missing or worn morphology.

Institutional abbreviations

ALA-VP, specimens from the Middle Awash, Ethiopia; **AUH**, specimens from the Baynunah Fm., Abu Dhabi, U.A.E.; **BC**, specimens from the Chemeron Fm., Kenya; **EK**, specimens from Ekora, Kenya; **EP**, specimens from Laetoli, Tanzania; **ER**, specimens from the Koobi Fora Fm., Kenya; **KNM**, National Museums of Kenya; **KP** specimens from Kanapoi, Kenya; **L** followed by a number series, specimens housed in the National Museums of Ethiopia in Addis Ababa, from the Middle Awash or the Omo; **LAET**, specimens from Laetoli, Tanzania; **LT**, specimens from Lothagam, Kenya; **M** followed by a number series, specimens housed in the National Museum, London; **MMK**, specimens housed in the McGregor Museum, Kimberley, Cape Province, South Africa; **MNHT**, specimens housed in the Museum of Natural History, Tripoli, Libya; **NK**, specimens from the Nkondo Fm., Uganda; **NY**, specimens from the Kisegi-Nyabusosi area, Uganda; **TM,** specimens from Toros Menalla, Chad; **W** followed by a number series, specimens from Omo, Ethiopia; **WT**, specimens from West Turkana, Kenya; **YS**, specimens from Omo, Ethiopia.

Methods

Because of the size and weight of KNM-ER 63642, the dorsal and ventral halves of the cranium were three-dimensionally scanned separately while it was supported in plaster-and-burlap “jackets,” and the resulting files were “stitched” together by TGI to reproduce the specimen as a single entity. The scanner used was the Artec Eva to provide the initial images and the Artec Space Spider was used to capture extra details. Artec Eva’s 3D point accuracy is up to 0.1 mm and resolution is up to 0.5 mm. Artec Space Spider’s 3D point accuracy is up to 0.5 mm and resolution is as fine as 0.1 mm. The raw scans were captured, cleaned, aligned, processed, and finalized in Artec Studio software. Resulting output file formats are .stl without texture and .ply with vertex color. The texture resolution for both Artec Eva and Artec Space Spider is 1.3 mp.

Measurements were taken on the cranium with 2000 mm body calipers, 300 mm dial calipers with gradations of 0.05 mm, 100 mm digital calipers accurate to 0.01 mm, and using the measurement function in MeshLab on 3D scanned images

SYSTEMATIC PALEONTOLOGY

Class MAMMALIA Linnaeus, 1758
Order PROBOSCIDEA Illiger, 1811
Family ELEPHANTIDAE Gray, 1821
Genus *Loxodonta* F. Cuvier, in F. Cuvier & Geoffroy Saint-Hilaire, 1825 (anonymous emendation, 1827)

Loxodonta adaurora Maglio, 1970

Occurrence

Eastern Africa. Beden (1983) divided the species into time-successive subspecies, Pliocene *Loxodonta adaurora adaurora* and early Pleistocene *L. adaurora kararae*. Morphologically and temporally, the referred specimen belongs in the older subspecies. Along with its derivation from the Kanapoi Fm. at the type site of Kanapoi, Kenya, the older subspecies is documented in the Ekora Fm., Ekora, Kenya (Maglio, 1970, 1973), Mursi Fm. and Mb. B of the Shungura Fm., Omo, Ethiopia, (Beden, 1987a), Aramis and Baidareem Mbs. of the Sagantole Fm., Middle Awash, Ethiopia (Mebrate, 1983; Kalb & Mebrate, 1993), Kataboi and lower Lomekwi Mbs. of the Nachukui Fm., West Turkana, Kenya (Harris *et al.*, 1988), Moiti and Lokochot Mbs. of the Koobi Fora Fm., Allia Bay, Kenya (Beden, 1983), Lonyumun Mb. of the Koobi Fora Fm., Ileret, Kenya, Kaiyumung Mb. of the Nachukui Fm. (=Unit 3; Feibel, 2003; McDougall & Feibel, 2003), Lothagam, Kenya (Maglio, 1970, 1973; Maglio & Ricca, 1977; Coppens *et al.*, 1978), Chemeron Fm., Tugen Hills, Kenya (Maglio, 1973; Hill *et al.*, 1985, 1986), and possibly in the Kanam Fm., Kanam East and West, Kenya (MacInnes, 1942; Maglio, 1973), the Sidi Hakoma and Denen Dora Mbs. of the Hadar Fm., Middle Awash, Ethiopia (White *et al.*, 1984), and Nkondo Fm., Western Rift, Uganda (Sanders, 1990; Pickford *et al.*, 1993).

Age

Loxodonta adaurora adaurora is early to late Pliocene in age (Sanders *et al.*, 2010; Sanders, 2020).

Revised diagnosis

(Based on Maglio, 1970, 1973; Maglio & Ricca, 1977; Beden, 1983; Harris *et al.*, 2003; Larramendi, 2016; Sanders, 2017, 2020). Cranial morphology resembles that of extant African elephants, but with longer, more vertically-oriented premaxillae (accentuating the effect of the anteroposterior compression of the cranium), broader forehead, more robust and distally flaring tusk alveoli, more extensive prenasal region, more anterior position of orbits, greater posterior projection of small-sized occipital condyles, broadest point of the occipital planum slightly above the level of the external auditory meatus, flatter external surface of the zygomatic arch, more prominent frontoparietal struts lateral to the nasal opening, and higher position of the nasal aperture above the level of the zygomatic process of the frontal. No occipitoparietal inflation, or “bossing.” Anteroposteriorly very short cranial vault posterior to the nasal bones. Cranial vault convex or flat transversely and longitudinally. Generally similar to extant African elephants in having crania with a relatively flat occipital planum angled anterosuperiorly, short, convex parietofrontal region, position and shape of fossa for the nuchal ligaments, orbital level lower than nasal aperture, and configuration of the temporal fossa. Mandibular morphology differs from that of extant African elephants by a longer symphysis with a more protuberant anterior “beak,” but is similar in relative length of the corpus, height of the articular condyle well above that of the coronoid process, and slight lateral eversion of the coronoid. Molars with a modest number of well-spaced, thick plates (plate formula is x8x–x10x in M3/m3), thick, unfolded enamel, and subhypsodont with height equal to or less than width. Molar plates transversely widest at their bases, with rounded, convex lateral borders gently convergent toward their apices. Unworn median conelets higher than lateral conelets. Anterior and posterior accessory conules large and free at their apical extremities, fused to plates with occlusal attrition and incorporated into prominent, rounded median loops of enamel wear figures. Differs from modern African elephants in lacking development of true loxodont sinuses in occlusal enamel wear figures. Apparent retention of upper and lower third and fourth permanent premolars. Plate formulae dP2/dp2, 3/?4; dP3/dp3, --/6; dP4/dp4, 8/7; P3/p3, 2/3; P4/p4, --/--; M1/m1, --/6; M2/m2, 6-7/7; M3/m3, 8–10/10. Tusks not spiraled but gently curved upward in a single plane, and reach very large girth and length. Contra Maglio (1970) and Beden (1983), vestigial incisive cavities and lower tusk alveoli are absent. Postcrania from the type and several other individuals represent very large elephants (estimated body mass nine tons and shoulder height 386 cm for the type specimen) and are most similar morphologically to those of African elephants.

Differential diagnosis

(Based on Arambourg, 1970; Maglio, 1970, 1973; Maglio & Hendey, 1970; Coppens, 1972; Maglio & Ricca, 1977; Beden, 1983, 1987a, b; Tassy, 1995, 2003; Mackaye 2001; Mackaye *et al.*, 2005, 2008; Sanders, 2007, 2010, 2011, 2020; Saegusa & Haile-Selassie, 2009; Sanders & Haile-Selassie, 2012). Morphologically recognizable from (1) late Miocene-early Pliocene stegotetrabelodont species by greater number of molar plates, higher lamellar frequency, U-shaped transverse valleys and corresponding parallel-sided plates in lateral view, greater molar crown height, more regular development of anterior and posterior accessory conules in third molars, thicker distribution of cementum on molar crowns, cross-sectionally more massive, curved upper tusks and absence of lower tusks, mandibles with higher rami and much shorter symphyses, and cranium with considerably more flared tusk alveoli; (2) late Miocene-early Pliocene *Stegodibelodon schneideri* by much shorter, distally narrower mandibular symphyseal spout, greater number of plates than in the Menalla-Toros Menalla-Kolinga 1, Chad molar sample (but not than in the Kollé, Chad sample), higher-crowned molars, parallel-faced plates separated by U-shaped transverse valleys; greater covering of cementum, and generally higher lamellar frequencies and thinner enamel (note that the edentulous mandible from the Adu-Asa Fm. in the Middle Awash, Ethiopia attributed to *Stegodibelodon schneideri* belongs in *Primelephas korotorensis* [see Saegusa & Haile-Selassie, 2009; Sanders *et al.*, 2010]); (3) early Pliocene *Selenetherium kolleensis* by shorter, more distally narrower mandibular symphyseal spout, greater development of accessory conules, convex-concave-shaped enamel wear figures, parallel-faced plates separated by U-shaped transverse valleys, higher molar crowns, higher lamellar frequencies, third molars with a greater number of plates, and lower range of enamel thickness (this species was originally subsumed into *S. schneideri* by Sanders *et al.* [2010], but its distinctive molar enamel wear figures and primitive number of molar plates warrant recognition of separate species status); (4) late Miocene-early Pliocene *Primelephas korotorensis* by greater number of molar plates, higher lamellar frequency, U-shaped transverse valleys and parallel-sided molar plates in lateral view, greater crown height of molars, more extensive distribution of accessory conules throughout molar crowns, thicker distribution of cementum, less pronounced projection of the mandibular symphyseal "beak," convex frontal, and relatively broader nasal aperture downturned laterally and situated higher relative to the orbits; (5) late Miocene "*Elephas" nawataensis* by a blunter, more downturned symphyseal "beak," dp4 with a greater number of plates, plate shape parallel-faced with U-shaped transverse valleys, and greater development of anterior and posterior accessory conules ("*E." nawataensis* exhibits no synapomorphies of *Elephas* and alternatively has been synonymized with *Primelephas korotorensis* because other than dp4 with a nascent sixth plate, its mandibular and molar morphology is identical to that of *P. korotorensis* [Sanders *et al.*, 2010]); (6) late Miocene "*Loxodonta"* sp. A "Lukeino-type" from Toros Menalla, Chad by less offset, less undulated incorporation of stronger anterior and posterior accessory conules into M3 enamel wear figures, more parallel-sided plates in lateral view, higher lamellar frequency, greater hypsodonty, thinner enamel, more gradual progression of plate sides from cervix to apex, and thicker distribution of cementum (there are no obvious *Loxodonta* synapomorphies associated with this part of the Toros Menalla elephant assemblage and therefore its assignment to *Loxodonta* should be considered very tenuous); (7) late Miocene "*Loxodonta*" sp. C by M3 with higher lamellar frequencies, thinner enamel, lower absolute molar crown height, and greater expression of anterior and posterior accessory conules throughout molar crowns, and smaller third molars (*Mammuthus subplanifrons* was inaccurately synonymized into "*L.*" sp. C by Mackaye [2001], but although m3s have the same plate number as *M. subplanifrons* they are far more hypsodont, larger, and have lower lamellar frequencies; moreover, there is nothing in the occlusal morphology of these Toros Menalla molars that is apomorphic of *Loxodonta*); (8) late Miocene-early Pliocene *Loxodonta cookei* by higher-crowned molars with more plates, no incipient development of median loxodont sinuses, U-shaped transverse valleys, and smaller permanent third premolars; (9) late Miocene-early Pliocene *Mammuthus subplanifrons* by greater lamellar frequency, higher molar crowns, greater distribution of accessory conules throughout molar crowns, thinner enamel, thicker distribution of cementum, lateral plate profiles more parallel-sided and not as bulbous, tusks not longitudinally torqued, mandibular corpus dorsoventrally thicker, and masseteric fossa of the ramus more extensive; (10) early Pliocene "*Elephas" ekorensis* by fewer molar plates, lower molar crown height, and cranium lacking incipient occipitoparietal "bossing" and with more divergent tusk alveoli (see "*E." ekorensis* section below); (11) Pliocene *Elephas recki brumpti* by lower molars with fewer plates, lower lamellar frequency, molar plate sides not rectilinear, fewer conelets per plate, thicker, unfolded enamel, mandible with longer, less rounded corpus in cross-section and more anteriorly projecting symphysis, cranium relatively longer, orbits less laterally flaring, lower relative to the nasal aperture, and more posteriorly situated in relation to tooth row, flat or convex vault with no occipitoparietal "bossing" or inflation of the occipital planum, and occipital planum relatively higher (alternatively, Zhang [2020] placed *E. recki brumpti* into *Phanagoroloxodon planifrons*, with *L. adaurora kararae* [see below]); (12) from "*Loxodonta"* sp. B "Kolle-type" by greater expression of anterior accessory conules and distribution of anterior and posterior accessory conules throughout the length of molar crowns, but otherwise is not very different morphometrically (there are no obvious *Loxodonta* synapomorphies in this part of the Kollé assemblage and therefore assignment to *Loxodonta* is very tenuous); (13) Pliocene *Loxodonta exoptata* by lower crowned molars with fewer, broader plates, lower lamellar frequency, thicker enamel, and no formation of median loxodont sinuses in occlusal enamel wear figures; (14) mid- to late Pliocene *Mammuthus africanavus* by fewer m3 plates, molar hypsodonty index lower, plate sides more curved from base to apex, fewer conelets per plate, stronger development of accessory conules, tusks not doubly recurved upward and inward distally, and occipital planum angled forward superiorly; (15) ?late Pliocene to early Pleistocene *Loxodonta adaurora* *kararae* by M2s with fewer plates, third molars with fewer plates, greater expression and distribution along molar crowns of accessory conules, thicker enamel, no central folding of enamel, lower lamellar frequencies, lower hypsodonty indices, and cranium with higher placement of orbits, transversely straighter lower margin of the occipital planum (in ventral view), and less robust exoccipital ridges (alternatively, based on his interpretation of comparative cranial morphology, Zhang [2020] placed *L. adaurora kararae* along with *Elephas recki brumpti* in *Phanagoroloxodon planifrons*); and from (16) Pleistocene species of *Palaeoloxodon* by triangular rather than rectangular shape of the temporal fossa, more anterosuperiorly angled occipital planum, lack of a parieto-occipital crest and no overlap of a crest on the parietofrontal region of the vault, no inflation of the occipital planum, and rostrum not flared into a "bell" outline distally.

Holotype

KNM-KP 385, adult male partial cranium with left and right M3, associated mandible with left and right M3, and partial skeleton, Kanapoi Fm., Kanapoi, Kenya (Maglio 1970).

Referred specimen

KNM-ER 63642, adult male cranium with left and right M2-3, lower Lonyumun Mb., Koobi Fora Fm., Ileret, Kenya.

Description

Cranium KNM-ER 63642 is well-preserved, largely undeformed, and missing only its nasal bones, tusks, left zygomatic arch, bullae, left occipital condyle, and part of the left lower corner of the occipital planum. Bone is eroded in the basicranial region and posterior to the third molars in the area of the broken pterygoid plates, and some step fracturing has occurred in the rostral trough. Despite the absence of or damage to these parts of its anatomy, KNM-ER 63642 is the most complete adult elephant cranium known from the late Miocene–early Pliocene interval. It is a massive specimen, of great length, height, and breadth, with a prominently elongate lower face (Table 1). Its impressive size and the girth of its incisor alveoli indicate that it belongs to an adult male individual.

Dentition **(Figure 4A-C).** On its left side, the cranium has a complete but deeply worn M2 and complete M3 with occlusal wear across its first four plates (Figure 4A). The M3 had not completely vertically descended into occlusion by the time of death. The right molars include a heavily abraded M2 that is worn away anteriorly and a complete M3 in the same condition as its left antimere. Modern African elephants in this phase of tooth emergence and wear (stage XX) are 34 ± 2 years of age (Laws, 1966; Jachmann, 1988), or perhaps slightly younger, between 30 to 32 years of age, based on known ages of modern African elephants with this degree of molar progression (Lee *et al.*, 2011). The enamel loops in the M2s are nearly obliterated by wear and only remnants of their outlines are preserved to indicate a plate formula of 7x.

The plate formulae for the third molars varies between 9x and x9x. In the left M3, plate 8 is offset lingually between plates 7 and 9, but constitutes a complete lamella. Greatest width of the third molars occurs at the base of the third or fourth plates. In transverse cross-section, the plates curve inward gradually toward their apices, providing the molars with a bowed, rounded profile (Figure 4B). In lateral view, the plates are parallel-sided, curve slightly forward at their apices, and are separated by U-shaped transverse valleys that are filled with cementum (Figure 4C). On the right side, unworn posterior plates of M3 are also individually covered with cementum. Spacing and anteroposterior thickness of plates yield a moderately low lamellar index (Table 2). In the occlusal wear figures, enamel is unfolded or weakly undulated and thick (Table 2). Where it is possible to observe, each plate is comprised of three to six conelets. In unworn plates, conelets are higher centrally than laterally. Anterior and posterior accessory conules are incorporated into enamel loops in the first few, worn plates, but only the first plate of the right M3 exhibits a pseudoloxodont enamel wear figure and there are no true loxodont sinuses (<> enamel loop wear figures). The M3s are very broad; the ratio of crown height to width is subhypsodont (Table 2). The preservation of these molars in the cranium are critical for confirming its taxonomic identity; morphologically and metrically they closely match M3s of other *Loxodonta adaurora* individuals (Table 2).

Anterior view **(Figure 5A).** In this aspect, the cranium has a rectangular shape dominated by the great length of the lower face (Table 1), which is comprised of elongate premaxillary bones that sheath the tusks. These long, distally divergent alveolar tubes flank a capacious external incisive fossa. The fossa is vertically tear-drop-shaped, broader and shallower inferiorly. The midline premaxillary suture is patent. Superiorly, the nasal processes of the premaxillaries are broader and flatter than their alveolar processes, and form an extensive bony planum on each side, inferior to the nasal aperture. The premaxillary nasal processes are bounded laterally by the roughened, swollen frontal processes of the maxillae.

The nasal aperture is broad and slightly downturned at its lateral margins. Its anteroposterior length is exaggerated by the disarticulation and consequent loss of the nasal bones along their frontal sutures. Internally, a prominent flat plate of bone, the nasal step of the premaxilla, is present laterally on each side. The aperture is located higher on the cranium than the orbits, which are relatively large and face primarily laterally. It is separated from the incisive fossa by a transverse bridge of bone that has a small, inferiorly projecting midline crest (the posterodorsal process of the premaxilla [Tassy, 1995]). Biorbital width is very broad and slightly greater than the breadth of the occipital planum (Table 1). The frontal borders the nasal aperture laterally on each side as stout struts which angle downward and outward to the orbits and upward and inward to the vault. The lateral edges of these struts demarcate the medial, superior edges of the temporal fossae. More posteriorly, the frontal and parietals form a very short cranial roof that is transversely and anteroposteriorly slightly convex. This view shows that there is no midline depression in the nuchal crest and no "bossing" or supralateral inflation of the parietals. The infraorbital foramina are hidden in anterior view, as they are inset deeply under the protuberant ventral processes of the orbits.

Posterior view **(Figure 5B).** On the left side, the posterior aspect of the cranium is missing part of its exoccipital, adjacent temporal squamous contribution to the occipital planum, and occipital condyle. Nonetheless, the overall configuration of the occipital planum is well-defined. It is lightly rounded superiorly with no midline depression, and is rounded superolaterally. The occipital planum is broader than high, and is widest above the level of the external auditory meatus at the lower lateral edge of the nuchal crest on the supraoccipital. The supraoccipital is slightly wider than the exoccipital (observable on the right side) and relatively extensive.

Table 1. Comparative cranial dimensions of KNM-ER 63642 and other late Miocene-early Pliocene elephants. The measurement abbreviations and definitions are from Beden (1983). Abbreviations: e., estimated; +, indicates missing morphology and that the dimension was originally greater. All dimensions are in mm.

Abbreviation/ Measurement	**Specimen numbers, taxa, and provenience**					
	KNM-ER 63642 ***Loxodonta adaurora*** **Ileret**	KNM-KP 385 *Loxodonta adaurora* Kanapoi (type)	Y.S.69. 3213 *Loxodonta adaurora* Mursi Fm. (Beden, 1983)	KNM-KP 30204 *Loxodonta adaurora* Kanapoi	MNHT (VJM SSLM 301) *Stegotetrabelodon syrticus* Sahabi, Libya (Petrocchi, 1954)	AUH 502 *Stegotetrabelodon emiratus* Baynunah Fm. (Tassy, 1999)
La, maximum length along sagittal axis, dorsal, nuchal crest to distal premaxillary	**1367**	+1130	--	1370	+1340	--
Lc, length of cranial vault, nasal aperture to nuchal crest	**360**	--	--	--	--	--
Ld, length, nasal aperture	**left, 205; right, 201**	--	--	--	--	--
Le, length of premaxilla along sagittal axis	**932**	--	--	--	--	--
Lf, length, ventral, condyle to incisor alveolus	**1205**	e.1380	--	--	--	--
Lg, sagittal length from anteriormost molar alveolus to palatine spine	**326**	--	230	--	--	300
Lh, length, palatine spine to foramen magnum	**--**	--	320	--	--	300
Lj, length, palatine spine to basisphenoid spine	**--**	--	290	--	--	--
Lk, length, pterygoid process to foramen magnum	**--**	--	180	--	--	--
la, maxium width occipital planum	**811**	--	--	--	970	--
lb, minimum width between temporal lines	**426**	--	--	--	--	--
lc, biorbital width across postorbital processes	**845**	--	--	870	--	--
ld, minimum width across premaxillae at their bases	**624**	--	--	--	--	--
le, width across premaxillae at their premaxillary-maxillary sutures	**660**	--	--	--	--	--
lf, maximum width across premaxillae at their distal extremities	**827**	--	--	840	--	--
lg, width of nasal process	**--**	--	--	--	--	--
lh, width nasal aperture	**560**	--	--	--	--	--
lj, width across nuchal ligament fossa	**228**	--	--	--	--	--
ll, width of foramen magnum	**--**	--	--	--	--	--
ln, width between external auditory meatus	**e.764**	--	--	--	--	--
lo, width between lateral borders of glenoids	**e.739**	--	--	--	--	--
lp, width between medial borders of glenoid surfaces	**--**	--	355	--	--	--
lq, Bizygomatic width	**e.914**	--	--	--	1030	e.820
lr, width between anterior end of M2s	**26**	65	80	85	--	--
ls, width between poster end of M3s	**148**	--	190	--	170	--
lt, width between external edges of alveolar margins	**363**	--	295	240	--	--

Table 1 (continued). Comparative cranial dimensions of KNM-ER 63642 and other late Miocene-early Pliocene elephants. The measurement abbreviations and definitions are from Beden (1983). Abbreviations: e., estimated; +, indicates missing morphology and that the dimension was originally greater. All dimensions are in mm.

Abbreviation/ Measurement	**Specimen numbers, taxa, and provenience**					
	KNM-ER 63642 ***Loxodonta adaurora*** **Ileret**	KNM-KP 385 *Loxodonta adaurora* Kanapoi (type)	Y.S.69. 3213 *Loxodonta adaurora* Mursi Fm. (Beden, 1983)	KNM-KP 30204 *Loxodonta adaurora* Kanapoi	MNHT (VJM SSLM 301) *Stegotetrabelodon syrticus* Sahabi, Libya (Petrocchi, 1954)	AUH 502 *Stegotetrabelodon emiratus* Baynunah Fm. (Tassy, 1999)
lu, width across internal choanae	**108**	--	110	80	--	90
lv, minimum width across interalveolar crests	**71**	--	50	--	--	--
Aa, length, anteroventral border of external auditory meatus to most elevated part of temporal fossa	**408**	--	--	--	--	--
Ab, length, anteroventral border of external auditory meatus to most ventral edge of orbit	**454**	450	--	--	--	--
Ac, maximum height of orbit	**256**	150	--	180	--	--
Ad, height from alveolar border to top of temporal line	**e.727**	--	--	--	--	--
Ae, length, pterygoid process to anterior tip of premaxilla	**792**	770	--	760	--	--
Af, length, pterygoid process to postorbital process	**514**	500	--	500	--	--
Ag, height, pterygoid process to nuchal crest	**750**	--	--	--	--	--
Ah, length, pterygoid process to posterior edge of occipital condyle	**397**	340	--	--	--	--
Ba, length, temporal foramen	**230**	220	--	--	--	--
Bb, width temporal foramen	**250**	170	--	--	--	--
Bc, minimum length between occipital condyle and glenoid	**218**	--	--	--	--	--
Bd, minimum length between foramen magnum and anterior edge of auditory bulla	**--**	--	--	--	--	--
Be, width, tympanic process of squamosal	**--**	--	--	--	--	--
Bf, maximum width, auditory bulla	**--**	--	--	--	--	--
Bg, width, auditory bulla	**--**	--	--	--	--	--
Ha, height, condyles to top of nuchal crest	**662**	+290	--	--	--	--
Hb, height, top of nuchal ligament fossa to top of nuchal crest	**97**	--	--	--	--	--
Hc, height, nuchal ligament fossa	**260**	--	--	--	--	--
Dap, anteroposterior length, tusk alveolus opening	**left and right, 190**	left, 180	--	--	--	--
Dt, width, tusk alveolus opening	**left and right, 230**	left, 180	--	--	--	--
Glenoid width	**175**	--	--	--	--	--
Glenoid length	**80**	--	--	--	--	--
Zygomatic arch height	**65**	--	--	--	140	--
Zygomatic arch width	**31**	--	--	--	--	--

The occipital condyle is small (Table 2), ovoid in shape, and is situated well above the level of the palate. In contrast, the occipital region is dominated by the large extent of the fossa for the ligamentum nuchae. The fossa is located superiorly in the upper half of the planum. It is moderately deep, with a narrow sagittal crest in its midline. The fossa has the outline of a tall rectangle. Above and below the fossa, the planum is depressed relative to areas lateral to the fossa. Nonetheless, the occipital planum is mostly flat and has no inflation or occipitoparietal "bossing" superiorly.

Lateral views **(Figure 6A, B).** The most striking features of the cranium in lateral view are its height, anteroposterior compression, disproportionately long face compared to the relatively very short vault, and elevation of the preserved occipital condyle and basicranium substantially above the level of the palate. The orbit is located in vertical line above the anterior of M2 and below the level of the lower margin of the nasal aperture. It is bounded posteriorly by a raised portion of the zygomatic process of the maxilla, and by a distinct but not inflated zygomatic process of the frontal. A third process, the anterolaterally-projecting ventral process of the orbit, overhangs the infraorbital foramen and is located along the anteroinferior margin of the orbit, on each side of the cranium. The orbital fossa is relatively large and is oriented primarily laterally and slightly anteriorly.

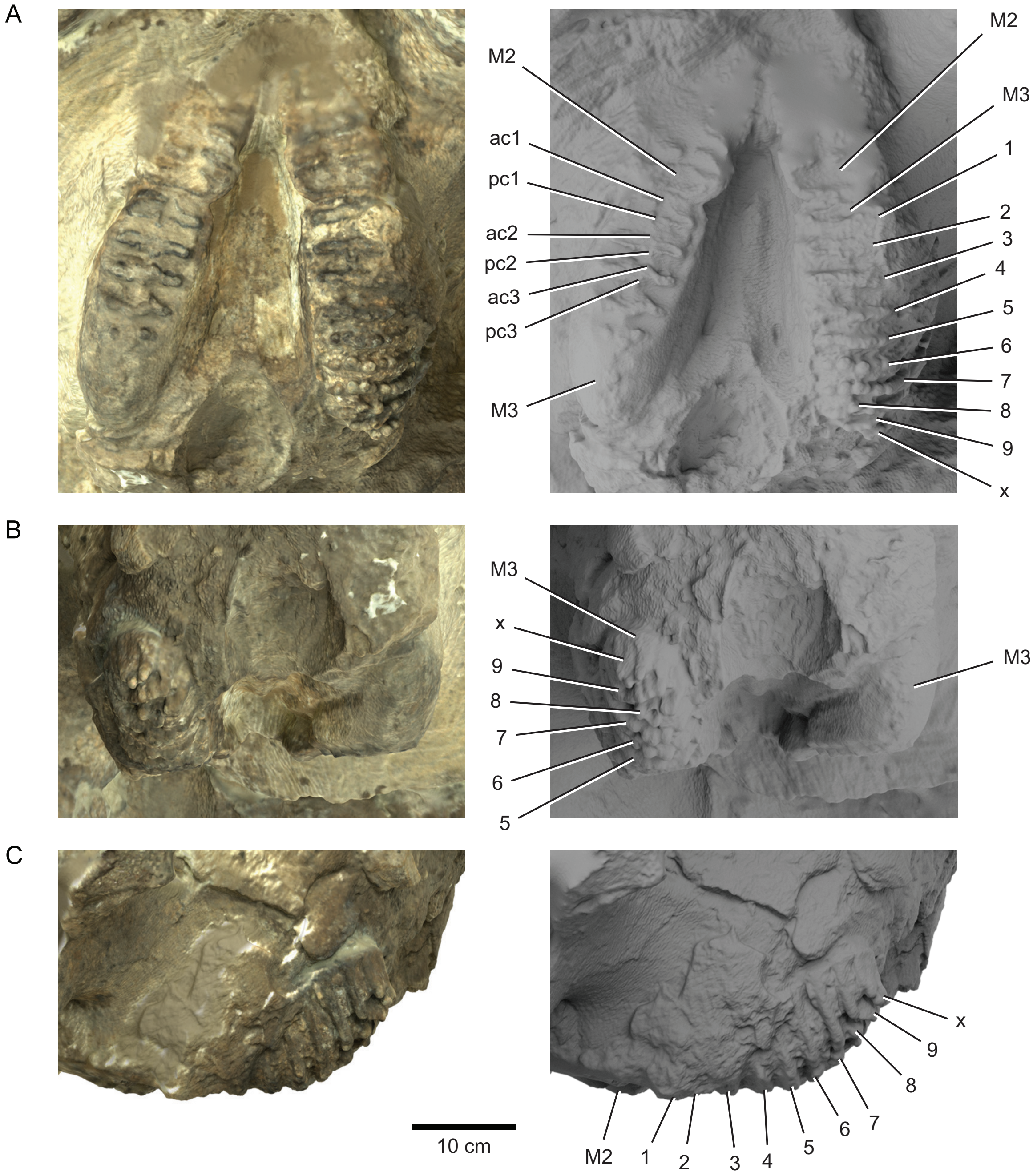

Figure 4. Left and right M2-3 of KNM-ER 63642, *Loxodonta adaurora*, from the lower Lonyumun Member of the Koobi Fora Formation, Ileret, Kenya. **A**, Occlusal view. **B**, Posterior view. **C**, Left lateral view. Abbreviations: ac, anterior pretrite accessory conule; M, upper molar; pc, posterior pretrite accessory conule; x, postcingulum or nascent last molar plate; 1, 2, 3, . . ., plate number, counted from the anterior end of the crown.

Table 2. M3 dimensions of KNM-ER 63642 and other African fossil elephants relevant for comparison. Abbreviations: e., estimated; ET, enamel thickness; H, crown height; HI, hypsodonty index, height x 100/width (<100, brachyodont; ≥100, hypsodont); L, molar length; LF, lamellar frequency, number of plates per 100 mm; n, number of individuals in sample; PF, plate formula; W, crown width; x, pre- or postcingulum(id); +, indicates missing morphology and that the dimension was originally greater. All dimensions are in mm.

Taxon/Molar/Specimen	**PF**	**LF**	**L**	**W**	**H**	**HI**	**ET**
Stegotetrabelodon emiratus							
M3 AUH 502 Tassy, 1999	5+	2.9	--	e.103.0	59.7	e.60.3	--
Stegotetrabelodon syrticus							
M3 (n=7) Petrocchi, 1943, 1954; Gaziry, 1987 (Sahabi)	6x to x6x	--	224.0-250.0+	103.0-125.0	66.0-78.0	62-64	--
Stegotetrabelodon orbus							
M3 (n=5) Sanders, in press (Nawata Fm.)	x6 to x6x	2.75-3.25	207.5-254.4	104.3-110.5	73.0-74.0	66-71	4.7-7.0
Stegodibelodon schneideri							
M3 (n=2) Coppens, 1972 (Kolinga, Chad)	x7x	2.5-3.0	300.0	110.0	78.0-87.0	71-79	5.0
M3 TM127.01.001 Mackaye, 2001; Mackaye *et al.,* 2005 (Toros Menalla, Chad)	+7x	2.9	+240.0	+103.0	60.0+	--	7.0
M3 (n=3) Mackaye, 2001; Mackaye *et al.,* 2005 (Kollé, Chad)	8x-x9x	3.3-3.5	+245.0-273.0	95.0-103.0	52.0-+55.0	51-52	5.0-6.0
Selenetherium kolleensis							
M3 (n=4) Mackaye *et al* ., 2005 (Kollé, Chad)	6x	2.1-3.0	210+	97.0-107.0	52.0+	49	5.5-7.5
Primelephas korotorensis							
M3 (n=22) Maglio, 1973; Mebrate, 1983; Kalb & Mebrate, 1993; Sanders, 1997; Mackaye *et al.,* 2008; Saegusa & Haile-Selassie, 2009	x7x-8x	3.1-4.1	197.2-268.0	83.5-104.5	53.0-72.0	51-76	3.4-6.1
Mammuthus subplanifrons							
l. M3 L27-1b Sanders, 2007 (Middle Awash)	+5+	3.5	+154.0+	102.0	91.0	89.0	4.0
r. M3 ALA-VP-2/309 Sanders, 2007 (Middle Awash)	9	--	--	87.0+	--	--	4.0-4.5
r. M3 MMK 4334 Sanders, 2007 (Vaal River)	+5x	3.3	+181.2	104.8	worn	--	4.3-4.7
l. M3 M 25160 Sanders, 2007 (Western Rift)	+3x	--	+112.0	104.0	worn	--	5.0-7.0
"Loxodonta" sp. A "Lukeino-type"							
M3 (n=4) Mackaye, 2001 (Toros Menalla, Chad)	x8x	3.0-3.7	+160.0-246.0	88.0-104.0	67.0-+83.0	74	5.0-6.0

Table 2 (continued). M3 dimensions of KNM-ER 63642 and other African fossil elephants relevant for comparison. Abbreviations: e., estimated; ET, enamel thickness; H, crown height; HI, hypsodonty index, height x 100/width (<100, brachyodont; ≥100, hypsodont); L, molar length; LF, lamellar frequency, number of plates per 100 mm; n, number of individuals in sample; PF, plate formula; W, crown width; x, pre- or postcingulum(id); +, indicates missing morphology and that the dimension was originally greater. All dimensions are in mm.

Taxon/Molar/Specimen	PF	LF	L	W	H	HI	ET
"*Loxodonta*" sp. C							
M3 (n=2)	x8x	2.7	319.0-324.0	119.0-124.0	108.0-113.0	91	6.0-7.0
TM 190.01.01							
Mackaye, 2001							
(Toros Menalla, Chad)							
Loxodonta cookei							
r. M3	x7 or 8	3.5	202.0	86.4	worn	--	--
NK 62'89							
Sanders, 2007							
(Nkondo Fm., Western Rift)							
r. M3	x7x	4.0	235.0	92.2	worn	--	4.0
KNM-BC 189							
Sanders, 2007							
(Chemeron Fm., Tugen Hills)							
Loxodonta adaurora							
r. M3	**x9x**	**--**	**247.6**	**118.4**	**+88.5**	**--**	**4.3-5.0**
l. M3	**x9x**	**4.0**	**247.4**	**119.3**	**102.0**	**85**	**4.3-5.0**
KNM-ER 63642							
r. M3	x8x	3.25	280.3	118.7	104.5	95	4.7-5.5
l. M3	x8x	3.25	291.5	110.5	--	--	3.5-5.0
KNM-KP 383							
r. M3	x9x	4.0	241.9	106.6	worn	--	4.3-5.3
l. M3	x9	4.0	235.1	109.0	worn	--	4.3-5.3
KNM-KP 385 (type)							
r. M3	9x	4.0	e.295.0	110.7	worn	--	4.5-4.6
KNM-KP 390							
r. M3	e.8x	3.5	256.0	92.0	worn	--	4.4-4.7
KNM-KP 30191							
r. M3	+8x	3.75	e.250.0	110.2	--	--	3.7-4.4
l. M3	+8x	3.75	e.250.0	110.8	90.1	81	3.7-4.4
KNM-KP 30204							
r. M3	9x	4.0	210.0	100.0	60.0+	60+	3.5-3.8
l. M3	9x	4.0	210.0	99.0	62.0+	63+	3.5-3.8
KNM-ER 346							
Beden, 1983							
(Kubi Algi Fm.)							
M3	10x	3.9	268.9	107.2	106.7	99	3.7-4.8
KNM-LT 353							
Maglio, 1973							
r. M3	x9+	--	232.3+	79.5	77.5	97	--
l. M3	x9x	--	223.0	76.3	--	--	--
KNM-ER 63491 (Moiti/Lokochot Mb., Koobi Fora Fm., Ileret)							
r. M3	x10x	4.5	263.0	94.0	--	--	5.2
KNM-ER 16830							
Harris *et al.,* 1988							
(lower Lomekwi Mb., West Turkana)							
M3	x9x	4.4	265.0	105.0	100.0	95	--
YS 1969 3213							
Beden, 1987b							
(Mursi Fm., Omo)							

Table 2 (continued). M3 dimensions of KNM-ER 63642 and other African fossil elephants relevant for comparison. Abbreviations: e., estimated; ET, enamel thickness; H, crown height; HI, hypsodonty index, height x 100/width (<100, brachyodont; ≥100, hypsodont); L, molar length; LF, lamellar frequency, number of plates per 100 mm; n, number of individuals in sample; PF, plate formula; W, crown width; x, pre- or postcingulum(id); +, indicates missing morphology and that the dimension was originally greater. All dimensions are in mm.

Taxon/Molar/Specimen	**PF**	**LF**	**L**	**W**	**H**	**HI**	**ET**
"Elephas" ekorensis							
r. M3	x11x	4.25	275.3	93.4	110.6	118	3.7-3.9
l. M3 KNM-EK 424 (type)	x11x	4.25	e.315.0	99.4	118.4	119	3.8
M3 W3 79 Beden, 1987a (Usno Fm., Omo)	+5+	--	+112.0+	102.0	105.0	103	3.5-4.0
M3 W 380 Beden, 1987a (Usno Fm., Omo)	x4+	--	111.0+	98.0	104.0	106	3.6-4.2
"Loxodonta" sp. B "Kollé-type"							
M3 (n=3) Mackaye, 2001 (Kollé, Chad)	9x	3.0-4.2	+120.0-223.0	90.0-140.0	+80.0-+94.0	96	4.0-6.2
Loxodonta exoptata							
M3 LAET 76-4558 Sanders, 2011 (Upper Laetolil Beds)	11x	--	250.0	93.2	100.0	111	3.4-3.8
M3 EP 1618/00 Sanders, 2011 (Upper Ndolanya Beds)	+12X	--	290.0	97.5	140.0	144	3.5
r. M3 KNM-WT 16458 Harris *et al.,* 1988 (lower Lomekwi Mb., West Turkana)	9	4.0	+223.0	91.0	--	--	3.6
Loxodonta adaurora kararae							
M3 KNM-ER 347 (subspecies type) Beden, 1983 (Upper Burgi Mb., Koobi Fora Fm.)	x10x	4.5-5.0	200.0-205.0	81.0-82.0	90.0	109-111	2.8-3.5
M3 Omo 20.4.1969.3206 Beden, 1987a (Mb. B, Shungura Fm., Omo)	x9	4.25	225.0	98.0	--	--	3.0-3.5

This view reveals that the tusk alveoli are strongly angled downward, at a steeper angle than the forward slope of the vault. The inferior-to-superior slope of the occipital planum is straight and angled forward. The occipital condyle is relatively small (Table 1) and projects posteriorly. Its superiormost surface is located in a line with the lower edge of the external auditory meatus. Anteroposteriorly, the basicranium is very short. The zygomatic arch is also relatively anteroposteriorly condensed, with a short suture between its squamosal and jugal portions. It is not massive in construction and anteriorly angles downward.

The lateral view of the cranium also shows that the alveolar portion of the maxilla is dorsoventrally deep, and that the temporal fossa is tall. In this perspective, the fossa is triangular in shape, higher than anteroposteriorly long, with a rounded rather than sharp demarcation from the top of the vault, and has a modest posterolateral sweep outward towards the squamous part of the temporal bone. The temporal fossa is not overhung by its lateral edges and there is no bulging or "bossing" of the nuchal margin. On each side, the orbits are positioned anterior to the maxillary-premaxillary notch.

Dorsal view **(Figure 7A).** The most salient features observable in the dorsal aspect of the cranium are the great breadth of the nasal aperture, the modest size of the temporalis foramen, the anterior flare of the tusk alveoli and external incisive fossa, the anterosuperior angulation of the occipital planum, and the very short anteroposterior dimension of the vault (Table 1). In this view, the nuchal crest is curved forward in the midline and bent posteriorly at its lateral edges. The vault is slightly convex anteroposteriorly and transversely. It is narrow relative to other aspects of the cranium, such as the anterior ends of the tusk alveoli (Table 1). The zygomatic arch is short anteroposteriorly, widest at its squamosal part, and does not flare outwardly. The occipital condyle projects posterior to the occipital planum (observable on the right side).

***Ventral view* (Figure 7B).** Ventrally, the molar rows are convergent anteriorly and the distance across the moderately shallow palate is broadest posteriorly. The posterior surface of the rostrum forms a wall fronting the palatal region. This view reveals the robustness of the tusk alveoli and great thickness of the rostrum at its distalmost end, along with its strongly vertical orientation. Although much of it is weathered away, the anteroposterior truncation of the basicranium is obvious. The opening to the choanae is relatively modest in size (Table 1) and oval in shape.

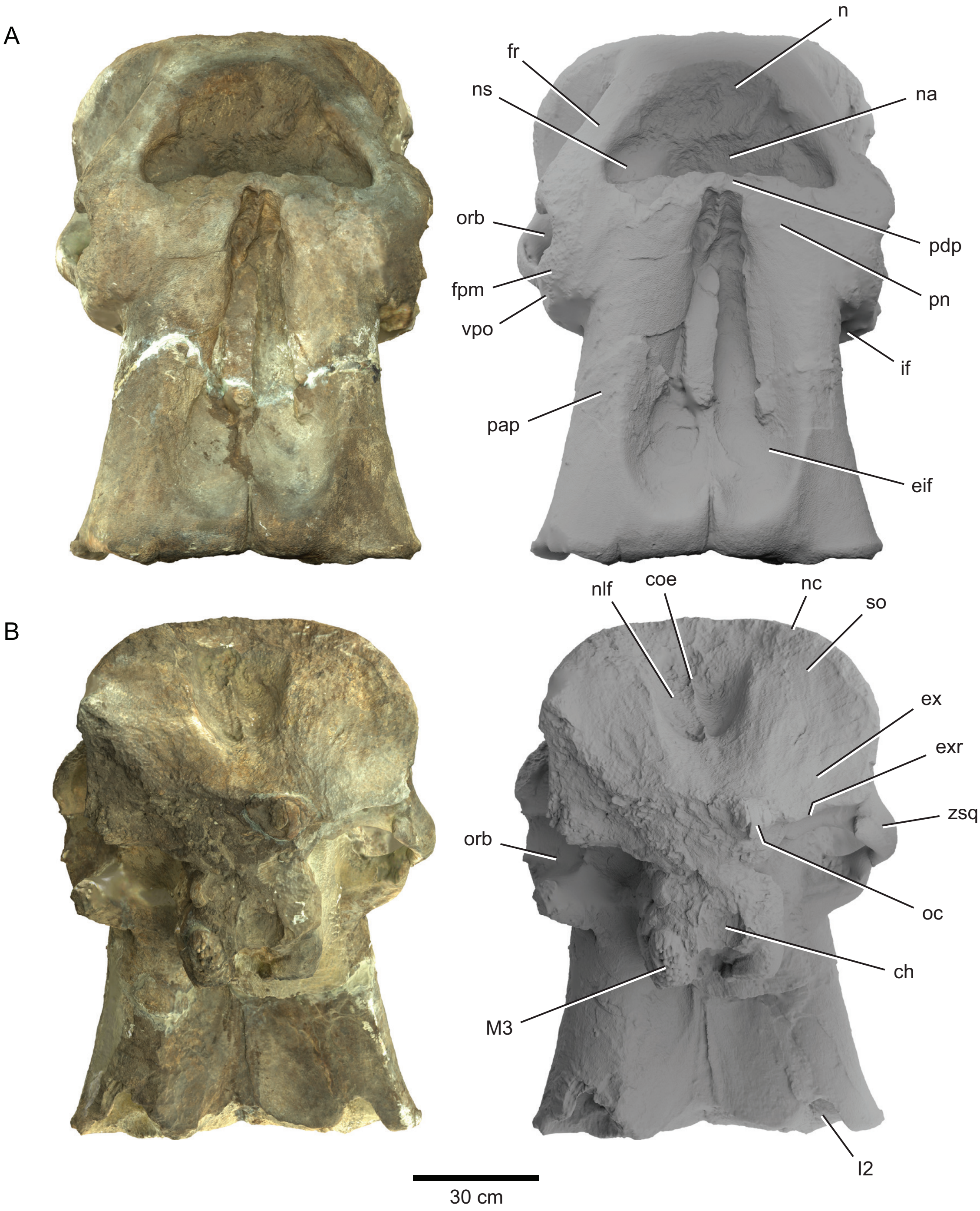

Figure 5. KNM-ER 63642, adult male cranium, *Loxodonta adaurora*, from the lower Lonyumun Member of the Koobi Fora Formation, Ileret, Kenya. **A**, Anterior view. **B**, Posterior view. Abbreviations for Figures 5–7: ch, opening to the choanae or nasal septum; coe, external occipital crest or ridge; eam, external auditory meatus; eif, external incisive fossa; ex, exoccipital; exr, exoccipital ridge; fpm, frontal process, maxilla; fr, frontal; gl, glenoid process; if, infraorbital foramen; I2, alveolus for upper tusk; mx, maxilla; M2, second upper molar; M3, third upper molar; n, nasal; na, nasal aperture; nc, nuchal crest; nlf, nuchal ligament fossa; ns, nasal step, premaxilla; oc, occipital condyle; orb, orbit; p, parietal; pap, alveolar process, premaxilla; pdp, posterodorsal process, premaxilla; pgf, postglenoid fossa; pn, nasal process, premaxilla; pzf, zygomatic process, frontal; pzm, zygomatic process, maxilla; so, supraoccipital; tf, temporalis foramen; tfs, temporal fossa; vpo, ventral process, orbit; zj, zygomatic arch, jugal segment; zsq, zygomatic arch, squamosal segment.

The ventral view vividly illustrates the relatively small size and square horizontal shape of the temporalis foramen. As well, this view encapsulates contrasting dimensions across various parts of the cranium, with bizygomatic width (inferred) > biorbital width > breadth of the occipital planum/braincase (Table 1). The glenoid is transversely concave and broad, anteroposteriorly convex and narrow, and has a shallow postglenoid fossa posterior to it. There is a distinct post-tympanic exoccipital ridge about 100 mm high and 230 mm wide on each side that posteriorly borders the narrow, transversely elongate auditory meatal passage. The deep inset of the infraorbital foramen under the orbit is also evident in this view.

Comparisons

Loxodonta adaurora. The metric and morphological features of craniodental specimen KNM-ER 63642 are consistent with its assignment to *Loxodonta adaurora*. It is the most complete adult elephant cranium known from the late Miocene to mid-Pliocene interval. Comparable specimens of *L. adaurora* include the partial cranium of the holotype, KNM-KP 385, from Kanapoi, Kenya, which is associated with a mandible and much of the postcranial skeleton (Maglio, 1970, 1973; Maglio & Ricca, 1977; Sanders, 2020). The type cranium is distorted and heavily damaged, especially dorsally, missing most of the vault, occipital planum, basicranium, and right side. It preserves the palate with right and left M3s, left occipital condyle, and

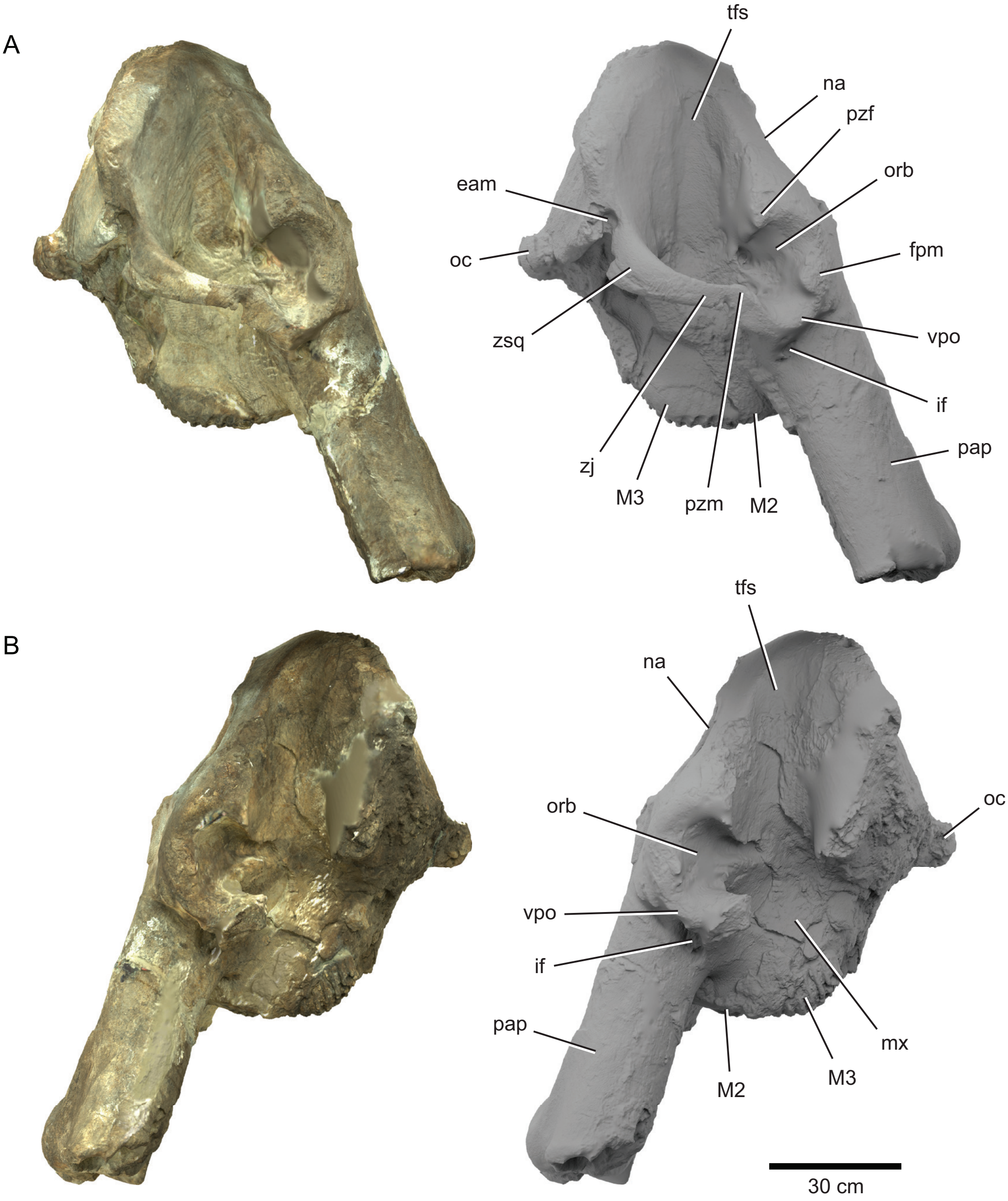

Figure 6. KNM-ER 63642, adult male cranium, *Loxodonta adaurora*, from the lower Lonyumun Member of the Koobi Fora Formation, Ileret, Kenya. **A**, Right lateral view, anterior is to the right. **B**, Left lateral view, anterior is to the left. Abbreviations are listed in Figure 5.

on the left side the zygomatic arch, glenoid, and premaxillary alveolar processes with the inserted proximal portion of a tusk. Prior to damage suffered in transport for study, the specimen was more complete (Harris *et al.*, 2003). The right condyle was originally present but is now missing.

Dimensions of KNM-KP 385 indicate that its cranium was similar in size to that of KNM-ER 63642 (Table 1). Based on the size of the molars and magnitude of the tusk cross-section, it belongs to a male individual. Of the cheek teeth, only the third molars remain, and the occlusal wear patterns of the m3s in the mandible suggest inclusion in Laws' (1966) mature adult age-grade group XXV or XXVI, between 47 and 49 ± 2 years of age at death (see also Lee *et al.*, 2011), older than individual KNM-ER 63642. Notable features of the cranium include long, robust, downwardly oriented and laterally-divergent tusk alveoli; zygomatic arch with a flat outer surface and no outward flare; small diameters of the temporalis foramen enclosed by the zygomatic arch; posterior projection of the occipital condyle; orbit anteriorly located and bounded by strong zygomatic processes of the frontal and maxillary; ventral process of the orbit overhangs the infraorbital foramen; and the orbital fossa faces primarily laterally and slightly anteriorly.

Morphological details of the type cranium from Kanapoi were merged with those of partial cranium KNM-LT 353 from Lothagam, Kenya to create a comprehensive reconstruction of the *L. adaurora* cranium (Maglio, 1970, 1973; Maglio & Ricca, 1977). However, the Lothagam cranial specimen is considerably younger in geological age (3.5–3.0 Ma)—hundreds of thousands of years—than the Kanapoi skull (4.2–4.1 Ma) (Coppens *et al.*, 1978; Feibel, 2003; McDougall & Feibel, 2003; McDougall & Brown, 2008; Sanders *et al.*, 2010; Brown & McDougall, 2011; Sanders, 2020) and only its left side is preserved. It is also missing most of its rostrum. Nonetheless, KNM-LT 353 exhibits many of the features that have been used to define the cranium of *L. adaurora*: overall, it is raised and anteroposteriorly foreshortened (although many elephant species, including *L. africana* and *L. cyclotis*, also have anteroposteriorly compressed crania, this feature is particularly exaggerated in adult male *L. adaurora* by the strong downturn of the rostrum and very short cranial vault);

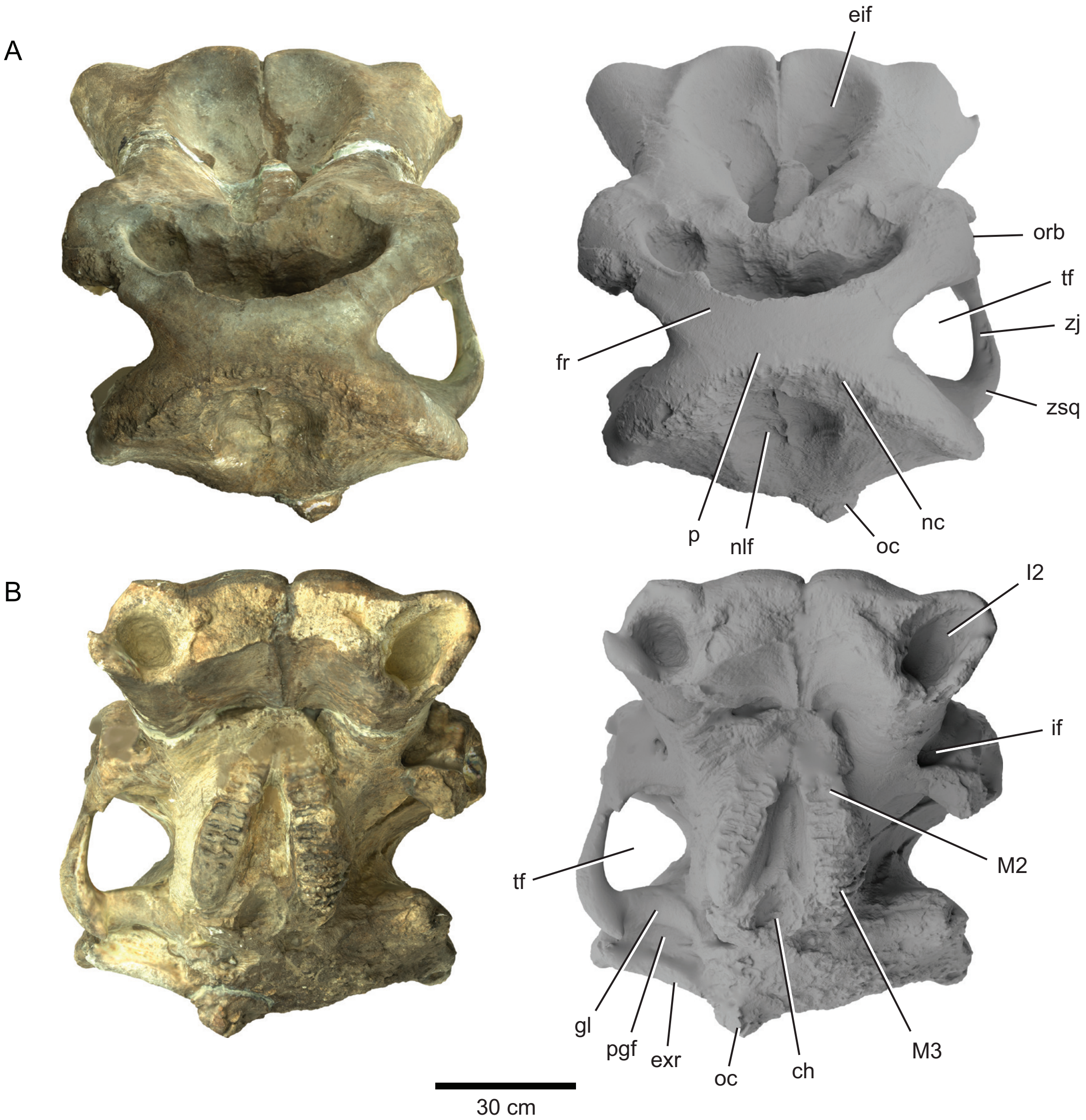

Figure 7. KNM-ER 63642, adult male cranium, *Loxodonta adaurora*, from the lower Lonyumun Member of the Koobi Fora Formation, Ileret, Kenya. Anterior is to the top. **A**, Dorsal view. **B**, Ventral view. Abbreviations are listed in Figure 5.

the occipital condyle is located considerably above the level of the palate and projects posteriorly beyond the occipital planum (contra Maglio & Ricca, 1977); the occipital planum is angled forward superiorly; the cranial vault is convex and demarcated from the temporal fossa by a rounded border; the zygomatic arch is laterally flat, short, relatively slender, does not project outwardly, and encloses a small temporalis foramen; the base of the rostrum is strongly downturned; the orbit is very forwardly positioned, in lateral view is anterior to the molars, and is bounded by strong but non-inflated zygomatic processes of the frontal and maxillary; the temporal fossa is relatively high and anteroposteriorly constricted; the nasal aperture is wide, slightly downturned at its lateral edges, and sits higher on the cranium than the orbits; the molar alveolar part of the maxilla is relatively deep beneath the zygomatic arch; the glenoid is broad, anteroposteriorly convex, and bilaterally concave; and there is no inflation or bossing of the occipital planum or parieto-occipital region. These features are all shared by the new Ileret specimen KNM-ER 63642. Unfortunately, Maglio (1970, 1973) and Maglio & Ricca (1977) did not provide dimensions of KNM-KP 385 or KNM-LT 353. The Lothagam partial cranium is now missing from the collections at the National Museums of Kenya in Nairobi.

Other Pliocene cranial specimens of *L. adaurora* include a large maxillary segment from below the level of the Allia Tuff at Allia Bay, Kenya that is heavily damaged but retains a well-preserved palate with dentition and associated left dentary, KNM-ER 346 (Beden, 1983), dated to 4.2–3.9 Ma (Beden, 1983; Harris, 1983; Brown, 1994; Coffing *et al.*, 1994; Leakey *et al.*, 1995; Bobe, 2011), a similarly preserved fragmentary cranium with a good palate and dentition from the ~4.2 Ma Mursi Fm., Omo, Ethiopia, Y.S. 1969 3213 (Beden, 1987a), a badly damaged cranium with third molars from the ~4.1 Ma Upper Deltaic Sands at Kanapoi, Kenya, KNM-KP 30204 (Harris *et al.*, 2003), and a palate with M3s from slightly <4.0 Ma Ekora, Kenya, KNM-EK 423 (Maglio, 1970; Behrensmeyer, 1976). Specimen KNM-ER 346 preserves morphological details that are important for systematic evaluation of *L. adaurora*, but which are eroded away in KNM-ER 63642. These include an overlap of the pterygoid process of the palatine covering the posterior edge of M3, and formation of the lateral edge of the internal nasal orifice by the pterygoid process of the sphenoid. As noted by Beden (1983), these features are shared with extant *L. africana* and differ from the condition in extant *Elephas maximus* and species of *Mammuthus*, in which the pterygoid process of the palatine is not exposed posteriorly. Status of tooth emergence in KNM-ER 346 indicates that this elephant was similar in age to the Ileret individual at time of death.

The Omo cranium exhibits the same arrangement of bones posterior to the last molar that are observable in KNM-ER 346. In addition, the internal nasal orifice is much longer than wide and oval in shape, and the occipital condyle appears to be located well above the level of the palate (Beden, 1983). This is a valuable specimen because it preserves auditory bullae and features of the basicranium, including foramina. The structure of the bulla in the Omo cranium and the position of its internal carotid foramen are very similar to the condition in extant African elephant crania (Van der Merwe *et al.*, 1995). Its M2 retains complete, individual enamel loops and M3 was just descending into occlusion at time of death, equivalent to Laws' (1966) age-grade group XVIII, 30 ± 2 years, or between 29 and 33 years according to Lee *et al.* (2011) in their revision of age assessment from teeth in African elephants. Metric comparison between Y.S. 1969 3213 and KNM-ER 63642 is limited because they do not preserve many of the same measurable parts (Table 1), but metric and morphological aspects of their molars, along with similar shape of their internal nasal orifices, are consistent with placement of both in *L. adaurora*.

A partial cranium from Kanapoi, Kenya, KNM-KP 30204, was identified as belonging to *L. adaurora* by Harris *et al.* (2003). Except for dimensions of the teeth, no details were provided about this specimen by these authors. It is slightly larger than the Ileret cranium (Table 1), which might be attributable to its greater ontogenetic age. It is difficult to assess age-grade status of KNM-KP 30204 in comparison with modern African elephants, but the ejection of the M2s and wear pattern of the M3s are concordant with Laws' (1966) age-grades XXIII-XXV, 43–47 ± 2 years of age at death, or between 38 and 56 years according to Lee *et al.* (2011). The M3s of KNM-KP 30204 are nearly completely emerged from their crypts and have at least five plates with some wear; the first two to three plates apically form complete enamel loops. The M3s are morphometrically similar to those of KNM-ER 63642 except for apparently having eight rather than nine plates, and a slightly lower lamellar frequency (Table 2). KNM-KP 30204 is heavily damaged, missing parts of the tusk alveoli, basicranium, occipital planum, right zygomatic arch, braincase and upper face. Nonetheless, it preserves features shared in common with the new Ileret cranium, including strong downward angulation of the rostrum, broadly splayed distal tusk alveoli, deep molar alveolar portion of the maxilla below the level of the zygomatic arch, infraorbital foramen tucked beneath the ventral process of the orbit, and non-flaring zygomatic arch which encloses a small temporalis foramen.

A small, juvenile partial cranium from Kanapoi, Kenya, KNM-KP 66240, is accessioned as *L. adaurora*. It is heavily damaged on its ventral aspect and does not preserve teeth or much of its rostrum. Its cranial vault is biconvex and demarcated from the temporal fossae by rounded margins. Possibly because of its young ontogenetic age, it differs proportionally from KNM-ER 63642 and the composite KNM-LT 353/KNM-KP 385 cranium, in having a relatively longer and transversely less constricted, or "waisted," braincase, lower height and less anteroposterior compression, and has a stronger anterior midline inflection of the superior nuchal margin and bean-shaped nasal aperture that is not downturned at its lateral margins. Alternatively, it could belong to a different species than *L. adaurora,* as "*Elephas" ekorensis* and *L. exoptata* are also documented at Kanapoi (Maglio, 1973; Harris *et al.* 2003; Sanders, 2020). While this juvenile cranium is potentially important for assessing ontogenetic morphological remodeling of elephant crania in the early Pliocene, it has limited utility for taxonomic assessment of KNM-ER 63642.

Loxodonta adaurora kararae. Beden (1983, 1987a) placed a few specimens from the Upper Burgi Mb. of the Koobi Fora Fm., Koobi Fora, Kenya and Mbs. B and E of the Shungura Fm., Omo, Ethiopia into a new, progressive subspecies of *L. adaurora*, *L. adaurora kararae*. The age of the specimens from Shungura Mbs. B and E are approximately 3.3 Ma and 2.4 Ma (see Levin *et al.*, 2011), respectively. The Upper Burgi Mb. specimens, including the subspecies type cranium, are approximately dated to 1.95–1.87 Ma (see McDougall *et al.*, 2011). The subspecies type cranium, KNM-ER 347, was originally allocated by Maglio (1971) to "*Elephas*" *ekorensis*, based on erroneous misidentification of field numbers and belief that it derived from the older Kubi Algi Fm. (Beden, 1983). This cranium is from a much smaller individual, possibly female, of similar ontogenetic age to KNM-ER 63642. It is heavily damaged dorsally and rostrally, with only the base of the tusk alveoli preserved and missing much of the braincase and upper occipital region, as well as the zygomatic arches. Similarities to KNM-ER 63642 include anterosuperior angulation of the occipital planum, no apparent development of occipitoparietal bossing, posterior projection of relatively small occipital condyles, divergent tusk alveoli, and an apparently short, convex or flat frontal (see Beden, 1983). It differs from KNM-ER 63642 in having a more robust exoccipital ridge, much lower orbits (well below the level of the occipital condyles), less transversely straight exoccipital margin (in ventral view), and third molars with more plates, thinner enamel, higher lamellar frequencies, lack of obvious development of accessory conules, less prominent median conelets, and widest point higher than the base of the crown (producing a different transverse molar profile than the rounded cross-section of *L. adaurora adaurora*, including KNM-ER 63642).

Alternatively, Zhang (2020) placed *L. adaurora kararae*, particularly KNM-ER 347, along with *E. recki brumpti*, notably cranium L.1.70 from the Omo Shungura Fm. (see Beden, 1987a), in *Phanagoroloxodon planifrons*. L.1.70 derives from unit Mb. B11 of the Shungura Fm., which would give it an age of approximately 2.9 Ma (see Levin *et al.*, 2011), a million years older than KNM-ER 347. Features used to support Zhang's (2020) allocation of KNM-ER 347 to *Ph. planifrons* are: Low position of the orbits close to the base of the tusk alveoli, marked post-temporal robusticity of the cranium, and the belief that asymmetry resulting from cranial distortion has produced an illusion of tusk divergence. These features are thought to resemble crania of *Ph. planifrons* from South Asia (Zhang, 2020). Firsthand investigation of the configuration of the left tusk alveolus of KNM-ER 347 shows that it is proximally angled away from the midline, and therefore that tusk divergence is real in this cranium. A more serious issue with Zhang's (2020) hypothesis is that cranium L.1.70 differs significantly from KNM-ER 347. It has nascent development of occipitoparietal bossing, parallel tusk alveoli, more protuberant orbits, and its orbits, while close to the base of the tusk alveoli, are not nearly as far below the level of the occipital condyles as those of KNM-ER 347. The Koobi Fora cranium differs substantially morphologically from KNM-ER 63642, and may not belong in *L. adaurora*; however, it is also unlikely to belong to the same species as cranium L.1.70.

"Elephas" ekorensis. An incomplete cranium from fossil beds at Ekora, Kenya, KNM-EK 422, was included in the original hypodigm of "*Elephas" ekorensis* (Maglio, 1970). This specimen is geologically younger than KNM-ER 63642, as the Ekora beds occur above a basalt dated to ca. 4.1 Ma (Brown & McDougall, 2011), though the faunal remains from the site have been considered contemporaneous with those of Kanapoi (Patterson *et al.*, 1970; Behrensmeyer, 1976). The Ekora cranium is heavily damaged, particularly rostrally and ventrally. Consequently, it is missing its tusks and molars. Comparison of the photographic image of the specimen (Maglio, 1970: pl. VII, fig. 21) with its current state of preservation shows that it suffered damage in research transport and subsequently had a heavy application of plaster around the posterior and lateral sides of the nasal aperture.

KNM-EK 422 was considered critical for placement of "*E." ekorensis* in *Elephas* (Maglio, 1970). KNM-EK 422 was described as having nascent development of traits more fully expressed in later species of *Elephas*, including modest dorsal and lateral expansion of the parietals, greatest width of the occipital planum at the level of the lateral expansion of the parietals, depression of the cranial apex in the midline, inflation of the occipital planum, parallel tusk sockets and inclination of the facial axis to the vertical axis of the cranium (Maglio, 1970; Maglio & Ricca, 1977). In addition, the nasal aperture does not appear to have been downturned at its lateral margins, and while the cranial vault is short, it is not as "waisted" transversely as in KNM-ER 63642. These features would differentiate the cranium of "*E." ekorensis* from that of *L. adaurora*, including KNM-ER 63642. Close examination of KNM-EK 422, however, does not support the morphological interpretations of it made by Maglio (1970) and Maglio & Ricca (1977). For example, there is no greater lateral or dorsal expansion of its parietals (no nascent parietal "bossing") than in *L. adaurora*; the nuchal crest is not depressed apically in the midline but posteriorly (as in *L. adaurora*); and the tusk sockets are largely broken away but are divergent at their proximal extent (see Maglio & Ricca, 1977). Traits that clearly differentiate *Elephas* from *Loxodonta*, such as parietal bossing, concavity of the cranial roof, and parallel tusk sockets (Todd, 2006), are not unambiguously present in KNM-EK 422.

Features that KNM-ER 63642 shares with other crania of *L. adaurora* are also present or ambiguous in KNM-EK 422. The cranial roof of KNM-EK 422 is flat to convex anteroposteriorly and bilaterally, the orbits are largely below the level of the nasal aperture, relatively large and face laterally and partly anteriorly, the frontoparietal border with the temporal fossa is rounded, the infraorbital foramen is hidden under the ventral orbital process, the exoccipital portions of the occipital are damaged, making it difficult to ascertain the widest part of the occipital planum, and the configuration of the frontal struts bordering the nasal aperture and premaxillary nasal processes are similar to the condition in KNM-ER 63642. KNM-ER 63642 does not resemble the defined morphology of the cranium of "*E." ekorensis* (e.g., Maglio, 1970; Maglio & Ricca, 1977). However, there is little to differentiate KNM-EK 422 from crania of *L. adaurora*, and thus no distinct evidence for allocating *ekorensis* to *Elephas*, even if morphometric features of isolated molars suggest that "*E.*" *ekorensis* is a slightly more advanced species than its contemporary, *L. adaurora* (Sanders, 2020).

A second cranium attributed to "*E." ekorensis* is that of a young juvenile, KNM-KP 30197 (Harris *et al.*, 2003). It is small but well preserved, though missing the zygomatic arches and requiring additional preparation, particularly to the basicranial region. The cranium has right and left worn dP2s, dP3s with all plates in wear and forming enamel loops, and emergent dP4s. In this specimen, the dP3s have six plates; on the right side this deciduous premolar measures L=70.5 mm x W=43.4 mm and has thin enamel (ET=1.7 mm). The central pillar of most plates is prominent but if there are accessory conules incorporated into the enamel wear figures, they are small and subtle (possibly doubled posterior to plate 4). The number of plates in dP3 is the same as in *L. adaurora* (Sanders, 2020), and the young age of the individual makes it unlikely that derived features were ontogenetically developed enough yet that they would yield more definitive grounds for identification. The absence of strongly expressed anterior and posterior accessory conules is probably the reason for the assignment of KNM-KP 30197 to "*E." ekorensis*. This specimen is too young to provide comparative information relevant for the identification of KNM-ER 63642.

Primelephas korotorensis. A heavily damaged partial cranium of the stem elephantine species *Primelephas korotorensis*, NY 46'92, was recovered from the late Miocene Lower Oluka

Fm. in the Kisegi-Nyabusosi area, Uganda (Tassy, 1995). It is missing nearly all of its rostrum, the braincase posterior to the parietofrontal suture, and its zygomatic arches. Primitively, the cranium retains P4s and its maxillary alveolar segment is not deep. Presence of M1s in wear and M2s still undescended indicate the juvenile status of this individual, equivalent to Laws' (1966) age-grade stage XI or about 15 ± 1 years at time of death, or 14 ± 1 years in Jachmann's (1988) recalibration of this age estimation technique, and 12.5–14.8 years according to Lee *et al.* (2011).

NY 46'92 is identified as *P. korotorensis* based on the morphometric features of its P4-M1s (Tassy, 1995; Sanders, 2017). Salient features of the partial cranium include broad, inflated nasal processes of the premaxillae lateral to the nasal aperture, a relatively small nasal aperture that is not downturned laterally, weakly divergent tusk alveoli, massive zygomatic process of the frontal, and derived elephantid features of a high basicranium (inferred from the angle of emergence of the M2s), anteroposteriorly short face, and loss of the dorsal opening of the infraorbital foramen (Tassy, 1995). In addition, Tassy (1995) claimed that the frontal is anteroposteriorly concave.

Some differences between NY 46'92 and KNM-ER 63642 may be associated with the younger age of the *Primelephas* individual (e.g., shallow maxillary alveolus and small, weakly diverged tusk alveoli). Other features of NY 46'92 may be autapomorphic (e.g., inflated premaxillary nasal processes) or have uncertain polarity compared with characteristics of KNM-ER 63642 and other elephants. For example, although the presence of a concave frontal is shared by species in the *Elephas-Mammuthus* clade, this feature was also claimed by Tassy (1995) to be present in a sister taxon to elephants, *Paratetralophodon* from the Siwaliks in Pakistan, and therefore its expression in *P. korotorensis* is not necessarily indicative of a close relationship between *Primelephas* and *Elephas* + *Mammuthus* (Tassy 1995). Moreover, if the frontal concavity is a primitive retention in *Primelephas*, it might indicate that the convexity of the frontal in *L. adaurora* is derived within Elephantidae (Tassy, 1995). It could also be autapomorphic and convergent on the condition in *Elephas* + *Mammuthus*. However, study of crania of *Paratetralophodon hasnotensis* (GSP 15032 and AMNH FM 19686) conversely indicates that the frontoparietal region is indisputably convex (pers. comm., H. Zhang). Furthermore, although firsthand examination of the *Primelephas* partial cranium NY 46'92 shows an anteroposterior concavity of the frontal towards the posterior break in the vault, it is not clear how much plastic distortion of the heavily damaged specimen contributes to that effect. Therefore, anteroposterior concavity of the frontoparietal region in *P. korotorensis* is an unreliable feature.

The palatal portion of a cranium of *P. korotorensis* preserving a right tusk alveolus was recovered from late Miocene Toros Menalla, Chad (Mackaye, 2001; Mackaye *et al.*, 2008). It retains few features in common with KNM-ER 63642 for comparison. The tusk alveolus measures a relatively modest 95 x 81 mm and appears to be non-flaring, more similar to the rostra of stegotetrabelodonts than those of *L. adaurora*. The very low-crowned M3s of this specimen, TM177-01-043, composed of only seven plates, also clearly differentiate it from *L. adaurora*, including KNM-ER 63642.

***Stegotetrabelodon* sp. nov. (Baynunah Fm.).**

Stegotetrabelodonts are late Miocene-early Pliocene stem elephantids characterized by numerous primitive dental features such as retention of lower tusks and P3-4/p3-4, very brachyodont molars with few loph(id)s or "plates," very thick enamel, pyramidal plate shape, low lamellar frequency, and weak covering of cementum (Maglio, 1973; Sanders *et al.*, 2010). The archaic nature of stegotetrabelodont gnathodental remains reflects their probable descent from an immediate precursor in the genus *Tetralophodon* (Markov, 2008; Sanders *et al.*, 2010; Wang *et al.*, 2017). Unfortunately, few stegotetrabelodont crania have been recovered to provide information about earliest elephant morphology to compare with KNM-ER 63642. Among these is an incomplete cranium, AUH 502, from the Baynunah Fm., Abu Dahbi, United Arab Emirates, dated biochronlogically to between 8.0 and 6.0 Ma (probably >6.5 Ma) (Bibi *et al.*, 2013; Sanders, in press). The Baynunah Fm. stegotetrabelodonts were placed by Tassy (1999) in *S. syrticus*, but are now assigned to their own species based on distinctive expression of accessory conules in their molars and differences in cheek tooth plate formulae (Sanders, in press).

AUH 502 is comprised of a partial cranium with right and left M1-2, an emerging left M3, and disarticulated right and left upper tusks. It is missing its rostrum and much of its posterior, upper lateral, and dorsal aspects. It is paired with crushed mandible AUH 503 that has a left lower tusk. Wear patterns of the molars and incomplete emergence of M3 place this individual in age category XVII, about 28 ± 2 years of age (Laws, 1966; Jachmann, 1988), or between 23 and 29 years according to the criteria of Lee *et al.* (2011). Because of weathering on the dorsal aspect of the cranium, it is impossible to ascertain its height. Nonetheless, it appears to have been anteroposteriorly compressed and probably dorsoventrally deep, as the basicranium is raised well above the level of the palate at an angle of about 50–60° (Tassy, 1999). In addition, the occipital condyles are small and do not appear to have projected posteriorly far beyond the occipital planum, the cranium is very broad (estimated to be ~820 mm across the zygomatic arches), the palate is shallow and broadest posteriorly, the zygomatic arch on the left side is not flared laterally and encloses a small temporalis foramen, the glenoid is saddle-shaped transversely and slightly convex anteroposteriorly, and the cranium has distinct postglenoid sulci. Its molars are far more primitive than those of *L. adaurora* (pentalophodont, very brachyodont M2s with pre- and posttrite accessory conules). The poor overall preservation of AUH 502 limits its utility for morphological comparison with KNM-ER 63642 and for establishing the primitive condition of cranial morphology in elephants.

***Stegotetrabelodon syrticus*.** A massive skull associated with a partial skeleton, MNHT (VJM SSLM 301), from late Miocene Sahabi, Libya (Warny *et al.*, 2003) includes a cranium that has suffered heavy weathering and loss of the brain case, nasals, orbital region, face, dorsum of the rostrum, and upper part of the occipital planum (Petrocchi, 1943, 1954). This damage makes impossible assessment of anteroposterior compression and height of the cranium. Nonetheless, a number of useful comparative observations may be made. It is massive in length and width (Table 1), with a broad, uninflated occipital planum, has a shallow fossa for the nuchal ligament that extends quite low on the occipital planum and small occipital condyles that project posteriorly, and exhibits a short, laterally flattened zygomatic arch. Drawings of the cranium in situ (Petrocchi, 1943) indicate a long, relatively narrow rostrum with non-divergent upper tusks exiting their alveoli in parallel. Based on the wear pattern of the m3s of the associated mandible, the Sahabi cranium is from a mature individual in age-grade stage XXV, 47 ± 2 years of age at death (Laws, 1966), or between 43 and 56 years according to the observations of Lee *et al.* (2011).

The M3s of the Sahabi specimen have fewer plates and are considerably more brachyodont than those in KNM-ER 63642, but these crania share some similarities (e.g., non-inflation of the nuchal planum, small size of the occipital condyles, great width of the cranium relative to overall size). Nevertheless, because of poor preservation of the specimen, comparison with the Ileret cranium is limited.

***Stegotetrabelodon orbus*.** Two very damaged and incomplete *S. orbus* crania are known from the late Miocene Lower Nawata Formation at Lothagam, Kenya (McDougall & Feibel, 2003). The first specimen, KNM-LT 26319, is best preserved on its ventral side, including right and left M2-3. It appears that the widest part of the cranium is at the squamosal end of the (missing) zygomatic arch. The glenoid is bilaterally broad and concave, and narrower and convex anteroposteriorly. Posterior to the glenoid is a deep, transversely elongate postglenoid sulcus. The condyles are relatively small and project slightly posterior to the occipital planum. The basicranium is short and raised. The rostrum is elongate, relatively narrow in ventral view, and from this perspective the tusk alveoli appear closely parallel to one another. It is possible that the dorsal view reveals more separation between the tusk alveoli and/or that they flared modestly distally, but it is clear that the overall configuration of the rostrum and tusk divergence were very different than the condition in KNM-ER 63642. The five plates of the M2s are occlusally worn into complete enamel loops followed by a postcingulum composed of four large conelets, and the M3s have four emergent plates with an additional half plate wedged buccally between plates 2 and 3. These molars are readily identifiable to species based on identification of posterior accessory conules throughout the M2 crowns, thick enamel, low lamellar frequency, and pyramidal shape of the plates in lateral view. Age-grade status based on the dentition of this individual is XIX, or 32 ± 2 years at death (Laws, 1966), which Lee *et al.* (2011) place within the interval 28–34 years in their revision of the technique.

The second specimen, KNM-LT 26318, is in far worse condition, heavily weathered, crushed into numerous fragments, and is missing its braincase, face, occipital region, and most of the rostrum. The basicranium is weathered and very compressed under the palate. The dorsal part of the skull is completely absent (Tassy, 2003). The alveoli for the M2s are mostly reabsorbed and the cranium exhibits poorly preserved M3s that are in wear anteriorly. The size of the M3s and depth of the maxillae suggest that the cranium is that of an adult male individual (Tassy, 2003), ontogenetically older than that of KNM-LT 26319. It is possible to observe that the rostrum is strongly downturned and that the orbit has a strong zygomatic process of the frontal, features that are shared with KNM-ER 63642, but proximally the tusk alveoli appear close to one another and are not divergent.

DISCUSSION

Taxonomy

Comparison of KNM-ER 63642 with late Miocene and early Pliocene African elephant crania reveal its identity as *Loxodonta adaurora*. Dentally, the M3s of the new cranium differ from those of more primitive elephants of the stegotetrabelodont-*Primelephas* grade by their higher crowns and greater covering of cementum, as well as by a greater number of parallel-faced plates separated by U-shaped transverse valleys. Molars of *L. adaurora* are also distinguished by regular expression of anterior and posterior central accessory conules throughout their crowns. They are equally distinguished from molars of *Mammuthus subplanifrons* and *L. cookei* by most or all of these features, and are less derived in plate formulae and hypsodonty than molars of "*Elephas" ekorensis* and *L. exoptata*. Morphometrically, they more closely resemble *L. adaurora* M3s from other sites (Table 2; Sanders, 2020). Numerous cranial traits of KNM-ER 63642 also clearly support this identification, including relative size, orientation, and architecture of the rostrum, circum-orbital morphology, position of the orbit relative to the nasal aperture, biconvexity and anteroposterior truncation of the parietofrontal vault, anterosuperior angulation of the occipital planum, and lack of inflation of the occipital planum and supralateral aspect of the parietals (Maglio, 1970, 1973; Maglio & Ricca, 1977).

In contrast, KNM-ER 63642 has important distinctions from crania of stegotetrabelodonts, most notably by the broad spacing and salient divergence of its tusk alveoli, and from the cranium of *Primelephas korotorensis*, particularly in the shape of the small nasal aperture of the Ugandan partial cranium, robustness of its premaxillary nasal processes, poorly diverged tusk alveoli, and possible anteroposterior frontal concavity (Tassy, 1995). There are also differences between KNM-ER 63642 and the described morphology of the cranium of "*E." ekorensis*, KNM-EK 422, which was detailed as having nascent parietal "bossing," a midline nuchal concavity, and non- or weakly-divergent tusk alveoli (Maglio, 1970, 1973; Maglio & Ricca, 1977). Re-examination of this specimen, however, does not demonstrate the unequivocal presence of these features. Without molars, it is impossible to definitively classify KNM-EK 422, which is little differentiated morphologically from crania of *L. adaurora*. Cranial remains are unknown for other late Miocene-early Pliocene elephant taxa. Nevertheless, the available comparative craniodental evidence is sufficient to place KNM-ER 63642 in *L. adaurora.*

It is difficult to test the hypothesis that *L. adaurora* belongs in *Loxodonta* (Maglio, 1970, 1973) because its molars do not display the loxodont sinuses in enamel loops typical of extant African elephants*,* and extant African elephants did not evolve the salient apomorphies that characterize *Elephas*, *Mammuthus*, and *Palaeoloxodon* (Lister *et al.*, 2005; Todd, 2006; Zhang *et al.*, 2018; Larramendi *et al.*, 2020). Parsimony analysis of elephant crania recovered *L. adaurora* and *L. africana* as sister taxa in a clade that is less transformed from the cranial morphology of the non-elephant outgroups *Gomphotherium angustidens* and *Paratetralophodon hasnotensis* than are crania of *Elephas*, *Mammuthus*, and *Palaeoloxodon* (Ferretti, 2016). More comprehensive parsimony analysis of elephant crania found tenuous support for *L. adaurora* as a basal member of the *Loxodonta* clade (Zhang, 2020). However, Zhang's (2020) study yielded very few features to validate placing *L. adaurora* in the same clade as extant African elephants, including a short frontal, distally flared tusk alveoli, and anterior inclination of the occipital planum, which would only justify the relationship if they are confirmed as synapomorphies rather than symplesiomorphies (Sanders, 2020; Zhang, 2020). The difficulty of assessing character state polarity of *L. adaurora* cranial features is compounded by the poor preservation or absence of crania in late Miocene elephants (e.g., stegotetrabelodonts, *Primelephas*, *M. subplanifrons*, *L. cookei*), although the relatively narrow spacing and lack of pronounced distal flare of tusk alveoli in *Stegotetrabelodon* and *Primelephas* suggest that rostral divergence might be synapomorphic for *Loxodonta*.

Reference to more distant outgoups may be more revealing. For example, a cranium of *Tetralophodon* sp. from early late

Miocene Morocco is strikingly complete (Geraads *et al.*, 2019) and has many features also retained in KNM-ER 63642, such as an anteroposteriorly short and biconvex parietofrontal, strong frontal struts lateral to the nasal aperture, a broad, laterally downturned nasal aperture located higher than the orbits, teardrop-shaped external incisive fossa, lack of supralateral inflation of the parietals and no inflation of the occipital planum, similar ovoid outline of the occipital planum, no midline depression of the nuchal margin, and similar development of zygomatic processes of the frontal and maxillary. The rostrum of this specimen, FSC-Sk-180, is elongate and reflected downward, but the tusk alveoli are parallel to one another and not distally flared, though are broadly separated dorsally by a well-delineated, tear-drop-shaped external incisive fossa. Unfortunately, because FSC-Sk-180 was a juvenile individual, with P4-M1 in wear and M2 emergent, it is impossible to gauge whether adult tusk alveoli in this species might have been more divergent. Also, its occipital planum is vertical and not superiorly angled forward. Height of an adult cranium attributed to *Tetralophodon*, from the late Miocene Samburu Hills, although heavily distorted, is reported to be steeply elevated (Nakaya *et al.*, 1987; Nakaya, 1994), and the cranium of *Paratetralophodon hasnotensis* from the Siwalik Series, Pakistan is raised, anteroposteriorly short in lateral view, and has a strongly upward-angled basicranium (Tassy, 1983, 1985). These observations, along with the limited morphological information from stegotetrabelodont crania, suggest that the morphotype of a raised, anteroposteriorly compressed cranium with an elongate rostrum is primitive for Elephantidae. From this slender evidence, much of the cranial morphology of KNM-ER 63642 and extant African elephants appears to be comprised of primitive retentions, although occipital planum angulation and tusk alveolar divergence cannot be dismissed as synapomorphies of the *Loxodonta* clade.

Additionally, post-alveolar palatine and pterygoid anatomy of the cranium obliterated by erosion in KNM-ER 63642 but preserved in partial crania of *L. adaurora* from Allia Bay, Kenya and Omo, Ethiopia are reliable synapomorphies of the clade (Beden, 1983; 1987a). As well, it is possible that, despite the lack of development of loxodont sinuses in enamel wear figures of *L. adaurora*, the existence of stout anterior and posterior central accessory conules throughout its molar crowns may constitute a synapomorphy of the clade, as may features of the postcranium (see Maglio & Ricca, 1977). Conversely, similarities between KNM-ER 63642 and species of *Palaeoloxodon* in rostral length and divergence are likely to be homoplasic, given the development of salient cranial apomorphies in the *Palaeoloxodon* clade (see Larramendi *et al.*, 2020) and their absence in KNM-ER 63642 and other crania of *L. adaurora*. It is doubtful that KNM-ER 63642 can provide resolution about genomic hypotheses concerning the relationship between *Palaeoloxodon* and *Loxodonta* (e.g., Meyer *et al.*, 2017).

Dietary adaptations

Dental isotopic studies of *Loxodonta adaurora* indicate that it was a grazer or mixed C_3-C_4 feeder that ate a substantial amount of C_4 plants (Cerling *et al.*, 1999; 2011a; Schoeninger *et al.*, 2003; Manthi *et al.*, 2017). Although there is no evidence for widespread open grasslands at the Pliocene sites it inhabited, the mixed feeding-grazing tendencies of *L. adaurora* fit with a trend in the greater Turkana Basin through the early Pliocene and younger intervals for decreasing woody canopy cover and increasing spread of C_4 vegetation (Levin *et al.*, 2011), and absence of significant forested or closed woody cover in the basin during the Pliocene (Cerling *et al.*, 2011b). Driven by selective pressures to efficiently utilize and compete for C_4 graze, the molars of *L. adaurora* evolved to be morphometrically more in phase with their feeding behavior than were those of late Miocene elephants. Consequently, their molars are composed of a greater number of plates and characterized by thinner enamel, closer spacing of parallel-faced plates separated by U-shaped valleys, thicker covering of cementum, and greater crown height approaching hypsodonty (Table 2; Sanders, 2020). These features were already in evidence in the dentition of >4.3 Ma *L. adaurora* specimen KNM-ER 63642.

Morphological features of the cranium identified by Maglio (1972) as important for enhancing effectiveness of fore-aft horizontal shearing in elephant mastication include those associated with maintaining uniform occlusal force across the molars and propelling a strong forward power stroke of the lower jaw. Elephant crania are typically more raised and anteroposteriorly shortened than those of gomphotheres, and in the mandibles of most elephants lower tusks are absent and the symphysis is foreshortened (Maglio, 1972, 1973). In consequence, the center of mass of the skull is more posteriorly located, over the mandibular coronoid process, and is vertically aligned with the direction of action of the temporalis muscles. As a functional result, contraction of the temporalis muscles does not interfere with the action of the superficial masseter muscles driving the forward power stroke of the lower jaw. Maglio (1972, 1973) also hypothesized that reorientation of the temporalis muscles in elephants was required to maintain even pressure on molars in occlusion.

Support for Maglio's (1972) hypothesis about the advantages of cranial and mandibular features in elephants for effective horizontal shearing can be found in convergent features of skull morphology of anancine gomphotheres and stegodonts. Both taxa also have brevirostrine mandibles lacking tusks, raised basicrania, in some species high, relatively anteroposteriorly foreshortened crania and evidently employed fore-aft (*Stegodon*) or obliquely-oriented (*Anancus*) horizontal shearing to masticate food; in addition, *Stegodon* spp. are convergent on elephants in having block-like molars formed of plates (Tassy, 1986; Hautier *et al.*, 2009; Saegusa, 2020). Dental isotopic studies of African *Stegodon kaisensis* reveal a shift from primarily browsing to grazing during the late Miocene to mid-Pliocene (Zazzo *et al.*, 2000), and anancine gomphotheres competed in Africa with elephants for grazing resources from their arrival on the continent in the late Miocene until their late Pliocene demise (Cerling *et al.*, 1999; Zazzo *et al.*, 2000; Kingston & Harrison, 2007; Levin *et al.*, 2008; Uno *et al.*, 2011; Roche *et al.*, 2013; Drapeau *et al.*, 2014).

It is difficult, however, to establish the timing of elephant cranial morphological reorganization as hypothesized by Maglio (1972), as the fossil record of adult elephant crania in the late Miocene and early Pliocene is very poor. Adaptations for proal masticatory action probably would have been less efficient in stegotetrabelodonts, because the great length of their symphyses and lower tusks (Petrocchi, 1943, 1954; Maglio, 1970, 1973; Tassy, 1999; Sanders, in press) would have located the center of mass of the skull more anteriorly than in elephantine elephants. In *L. adaurora*, the mandibular corpus and symphysis are slightly relatively longer than in extant African elephants (Maglio, 1970; Sanders, 2020), but the raised, anteroposteriorly compressed architecture of cranium KNM-ER 63642 and its vertically tall, anteroposteriorly restricted temporal fossae are modern in appearance, confirming details of a cranial composite (Maglio, 1970, 1973) that the species had evolved advanced adaptations for efficient proal employment of its molars. That cranial adaptations for horizontal shearing mosaically preceded the evolution of molar features advantageous for grazing, such as hypsodonty, greater number of plates, enamel folding, and thicker distribution of cementum, is indicated by evidence for high, anteroposteriorly compressed crania in late Miocene tetralophodontines and steeply raised basicrania in stegotetrabelodonts. The evident advantages of the craniodental adaptations of *L. adaurora* for eating C_4 grasses may explain why it was the dominant proboscidean in the greater Turkana Basin during the early to mid-Pliocene (Sanders, 2020).

ACKNOWLEDGMENTS

Permissions to study original fossil specimens in their care was provided by the following individuals and institutions: Graham and Margaret Avery (Iziko South African Museum, Cape Town, South Africa), Mark Beech (Coastal Heritage and Palaeontology Section of the Historic Environment Department, Abu Dhabi Tourism and Culture Authority, Abu Dhabi, United Arab Emirates), Amandus Kwekason and the late Michael Mbago (Tanzanian National Museums, Dar es Salaam, Tanzania), Meave Leakey (National Museums of Kenya, Nairobi, and Turkana Basin Institute, Ileret, Kenya), Adrian Lister and Jerry Hooker (The Natural History Museum, London), Emma Mbua, Fredrick Manthi, Mary Muungu, and Rose Nyaboke (National Museums of Kenya, Nairobi, Kenya), Muluneh Miriam (National Museum of Ethiopia, Addis Ababa, Ethiopia), and Ezra Musiime (Ugandan Museum, Kampala, Uganda). The figures were skillfully created and organized by scientific illustrator Carol Abraczinkas (University of Michigan Museum of Paleontology). Melissa Wood (University of Chicago Paleobiology Program) applied her expertise of Meshlab and Blender to convert images of KNM-ER 63642 from 3D .stl files for Figures 5-7. We are especially grateful to the field (Martin Kirinya, Shadrack Lomeiku Aburia, Apolo Alkoro Longaye, and Malmallo Longaye Letafua) and preparation laboratory (Ling'a Aike Milliamoi and Christopher Kiarie) teams of the Koobi Fora Research Project, Turkana Basin Institute (Ileret), preparators from the National Museums of Kenya (Robert Moru and Cliff Ochieng), and Steve Jabo (Smithsonian Institution Vertebrate Fossil Preparation Laboratory) for their careful and professional excavation, extraction, preparation, and conservation of the cranium. We are appreciative of the comments and suggestions of two anonymous reviewers, which have improved the content of the manuscript.

The project was funded by the National Geographic Society and additionally supported by ARTEC 3D (scanners and software), African Fossils, and the Turkana Basin Institute. Funding for research travel and site visits for WJS was generously provided by the Coastal Heritage and Palaeontology Section of the Historic Environment Department at the Abu Dhabi Tourism and Culture Authority (TCA Abu Dhabi), Meave Leakey and the Turkana Basin Institute, several Scott Turner Grants from the Department of Earth and Environmental Sciences, University of Michigan, and by grants to Terry Harrison (New York University, New York, NSF Grant BCS-0309513), and Carol Ward (University of Missouri, Missouri) and Fredrick Manthi (National Museums of Kenya) (NSF Grant BCS-1231749). Geological investigation of Area 14 by CSF was made possible by research funds from Rutgers University.

BIBLIOGRAPHY

Anonymous., 1827. Analytical Notices of Books. Histoire Naturelle des Mammifères, avec des Figures originale, dessinées d'après des Animaux vivans; &c. Par MM. Geoffroy-Saint-Hilaire, et F. Cuvier. Livraison 52 et 53. The Zoological Journal 3, 140-143.

Arambourg, C., 1970. Les Vertébrés du Pléistocène de l'Afrique du Nord. Archives du Muséum National d'Histoire Naturelle, Paris 7e Série, 10, 1-126.

Beden, M., 1983. Family Elephantidae. In: Harris, J. M. (Ed.), Koobi Fora Research Project. Volume 2. The Fossil Ungulates: Proboscidea, Perissodactyla, and Suidae. Clarendon Press, Oxford, pp. 40-129.

Beden, M., 1987a. Les Faunes Plio-Pléistocènes de la Vallée de l'Omo. Tome 2. Les Eléphantidés (Mammalia, Proboscidea). Éditions du Centre National de la Recherche Scientifique, Paris.

Beden, M., 1987b. Fossil Elephantidae from Laetoli. In: Leakey, M. D., Harris, J. M. (Eds.), Laetoli: A Pliocene Site in Northern Tanzania. Clarendon Press, Oxford, pp. 259-294.

Behrensmeyer, A. K., 1976. Lothagam Hill, Kanapoi, and Ekora: A general summary of stratigraphy and faunas. In: Coppens, Y., Howell, F. C., Isaac, G. L., Leakey, R. E. F. (Eds.), Earliest Man and Environments in the Lake Rudolf Basin. University of Chicago Press, Chicago, pp. 163-170.

Bibi, F., Hill, A., Beech, M., Yasin, W., 2013. Late Miocene fossils from the Baynunah Formation, United Arab Emirates. In: Wang, X., Flynn, L. J., Fortelius, M. (Eds.), Fossil Mammals of Asia. Neogene Biostratigraphy and Chronology. Columbia University Press, New York, pp. 583-594. https://doi.org/10.7312/columbia/9780231150125.003.0027

Bobe, R., 2011. Fossil mammals and paleoenvironments in the Omo-Turkana Basin. Evolutionary Anthropology 20, 254-263. https://doi.org/10.1002/evan.20330

Brown, F. H., 1994. Development of Pliocene and Pleistocene chronology of the Turkana Basin, East Africa, and its relation to other sites. In: Corruccini, R. S., Cichon, R. L. (Eds.), Integrative Paths to the Past. Paleoanthropological Advances in Honor of F. Clark Howell. Pentice Hall, Englewood Cliffs, N.J., pp. 285-315.

Brown, F. H., Feibel, C. S., 1986. Revision of lithostratigraphic nomenclature in the Koobi Fora region, Kenya. Journal of the Geological Society, London 143, 297-310. https://doi.org/10.1144/gsjgs.143.2.0297

Brown, F. H., McDougall, I., 2011. Geochronology of the Turkana Depression of northern Kenya and southern Ethiopia. Evolutionary Anthropology 20, 217-227. https://doi.org/10.1002/evan.20318

Cerling, T. E., Harris, J. M., Leakey, M. G., 1999. Browsing and grazing in elephants: The isotopic record of modern and fossil proboscideans. Oecologia 120, 364-374. https://doi.org/10.1007/s004420050869

Cerling, T. E., Harris, J. M., Leakey, M. G., 2003a. Isotope paleoecology of the Nawata and Nachukui Formations at Lothagam, Turkana Basin, Kenya. In: M. G. Leakey, M. G., Harris, J. M. (Eds.), Lothagam: The Dawn of Humanity in Eastern Africa. Columbia University Press, New York, pp. 605-624. https://doi.org/10.7312/leak11870-024

Cerling, T. E., Harris, J. M., Leakey, M. G., Mudida, N., 2003b. Stable isotope ecology of northern Kenya, with emphasis on the Turkana Basin. In: Leakey, M. G., Harris, J. M. (Eds.), Lothagam: The Dawn of Humanity in Eastern Africa. Columbia University Press, New York, pp. 583-594. https://doi.org/10.7312/leak11870-023

Cerling, T. E., Harris, J. M., MacFadden, B. J., Leakey, M. G., Quade, J., Eisenmann, V., Ehleringer, J. R., 1997. Global change through the Miocene/Pliocene boundary. Nature 389, 153-158. https://doi.org/10.1038/38229

Cerling, T. E., Levin, N. E., Passey, B. H., 2011a. Stable isotope ecology in the Omo-Turkana Basin. Evolutionary Anthropology 20, 228-237. https://doi.org/10.1002/evan.20326

Cerling, T. E., Wynn, J. G., Andanje, S. A., Bird, M. I., Korir, D. K., Levin, N. E., Mace, W., Macharia, A. N., Quade, J., Remien, C. H., 2011b. Woody cover and hominin environments in the past 6 million years. Nature 476, 51-56. https://doi.org/10.1038/nature10306

Coffing, K., Feibel, C., Leakey, M., Walker, A., 1994. Four-million-year-old hominids from East Lake Turkana, Kenya. American Journal of Physical Anthropology 93, 55-65. https://doi.org/10.1002/ajpa.1330930104

Coppens, Y., 1965. Les Proboscidiens du Tchad. Actes du Ve Congrés Panafricain de Préhistoire et de l'Étude du Quaternaire (Santa Cruz de Tenerife), I, 5, 331-387.

Coppens, Y., 1972. Un nouveau Proboscidien du Pliocène du Tchad, *Stegodibelodon schneideri* nov. gen. nov. sp., et le phylum des Stegotetrabelodontinae. Comptes Rendus de l'Academie des Sciences, Paris 274, 2962-2965.

Coppens, Y., Maglio, V. J., Madden, C. T., Beden, M., 1978. Proboscidea. In: Maglio, V. J., Cooke, H. B. S. (Eds.), Evolution of African Mammals. Harvard University Press, Cambridge, pp. 336-367. https://doi.org/10.4159/harvard.9780674431263

Cuvier, F., 1825. In: É. Geoffroy Saint-Hilaire and F. Cuvier (eds.), Histoire Naturelle des Mammifères, avec des figures originales, coloriées, dessinées d' après des Animaux vivans. Tome 6. A. Belain, Paris, pp. 117-118. https://doi.org/10.5962/bhl.title.78766

Drapeau, M. S. M., Bobe, R., Wynn, J. G., Campisano, C. J., Dumouchel, L., Geraads, D., 2014. The Omo Mursi Formation: a window into the East African Pliocene. Journal of Human Evolution 75, 64-79. https://doi.org/10.1016/j.jhevol.2014.07.001

Feibel, C. S., 2003. Stratigraphy and depositional history of the Lothagam sequence. In: Leakey, M. G., Harris, J. M. (Eds.), Lothagam: The Dawn of Humanity in Eastern Africa. Columbia University Press, New York, pp. 17-29. https://doi.org/10.7312/leak11870-002

Ferretti, M. P., 2016. A species-level phylogeny of elephants (Elephantinae, Proboscidea) based on cranial characters. Abstract, *26º* Giornate di Paleontologia 2016, Faenza.

Fortelius, M., Zliobaité, I., Kaya, F., Bibi, F., Bobe, R., Leakey, L., Leakey, M., Patterson, D., Rannikko, J., Werdelin, L., 2016. An ecometric analysis of the fossil mammal record of the Turkana Basin. Philosophical Transactions of the Royal Society B 371, 1-13. https://doi.org/10.1098/rstb.2015.0232

Gathogo, P. N., 2003. Stratigraphy and paleoenvironments of the Koobi Fora Formation of the Ileret Area, northern Kenya. M.S. Thesis. University of Utah.

Gathogo, P. N., Brown, F. H., 2006. Stratigraphy of the Koobi Fora Formation (Pliocene and Pleistocene) in the Ileret region of northern Kenya. Journal of African Earth Sciences 45, 369-390. https://doi.org/10.1016/j.jafrearsci.2006.03.006

Geraads, D., Zouhri, S., Markov, G. N., 2019. The first *Tetralophodon* (Mammalia, Proboscidea) cranium from Africa. Journal of Vertebrate Paleontology 39:3, e1632321.

Gray, J. E., 1821. On the natural arrangements of vertebrose animals. London Medical Repository 15, 296-310. https://doi.org/10.1080/02724634.2019.1632321

Harris, J. M., 1983. Background to the study of the Koobi Fora fossil faunas. In: Harris, J. M. (Ed.), Koobi Fora Research Project: Volume 2. The Fossil Ungulates: Proboscidea, Perissodactyla, and Suidae. Clarendon Press, Oxford, pp. 1-21.

Harris, J. M., Brown, F. H., Leakey, M. G., 1988. Stratigraphy and paleontology of Pliocene and Pleistocene localities west of Lake Turkana, Kenya. Contributions in Science, Natural History Museum of Los Angeles County 399, 1-128.

Harris, J. M., Leakey, M. G., Cerling, T. E., 2003. Early Pliocene tetrapod remains from Kanapoi, Lake Turkana Basin, Kenya. Contributions in Science, Natural History Museum of Los Angeles County 498, 39-115 (appendix by Winkler, A. J.).

Hill, A., Curtis, G., Drake, R., 1986. Sedimentary stratigraphy of the Tugen Hills, Baringo, Kenya. In: Frostick, L. E., Renaut, R. W., Tiercelin, J.-J. (Eds.), Sedimentation in the African Rifts. Blackwell and Geological Society of London Special Publication 25, Oxford, pp. 285-295. https://doi.org/10.1144/GSL.SP.1986.025.01.23

Hill, A., Drake, R., Tauxe, L., Monaghan, M., Barry, J. C., A. K. Behrensmeyer, A. K., Curtis, G., Jacobs, B. F., Jacobs, L., Johnson, N., Pilbeam, D., 1985. Neogene palaeontology and geochronology of the Baringo Basin, Kenya. Journal of Human Evolution 14, 759-773. https://doi.org/10.1016/S0047-2484(85)80058-0

Illiger, C. D., 1811. Prodromus systematis mammalium et avium additis terminis zoographicis uttriusque classis, eorumque versione germanica [Prelude to the systematics of mammals and birds with added zoographic terms of each class, and their German version]. Sumptibus C Salfeld, Berolini, Berlin. https://doi.org/10.5962/bhl.title.106965

Jachmann, H., 1988. Estimating age in African elephants: A revision of Laws' molar evaluation technique. African Journal of Ecology 26, 51-56.

Kalb, J. E., Mebrate, A., 1993. Fossil elephantoids from the hominid-bearing Awash Group, Middle Awash Valley, Afar Depression, Ethiopia. Transactions of the American Philosophical Society 83, 1-114. https://doi.org/10.2307/1006558

Kidney, C. L., 2012. Pliocene Stratigraphy and Geology of the Northeastern Ileret Region, Kenya. Master's Thesis, Department of Geology and Geophysics, University of Utah.

Kingston, J., 1999. Isotopes and environments of the Baynunah Formation, Emirate of Abu Dhabi, United Arab Emirates. In: Whybrow, P. J., Hill, A. (Eds.), Fossil Vertebrates of Arabia. With Emphasis on the Late Miocene Faunas, Geology, and Palaeoenvironments of the Emirate of Abu Dhabi, United Arab Emirates. Yale University Press, New Haven, pp. 354-372.

Kingston, J., 2011. Stable isotopic analyses of Laetoli fossil herbivores. In: Harrison, T. (Ed.), Paleontology and Geology of Laetoli: Human Evolution in Context. Volume 1: Geology, Geochronology, Paleoecology and Paleoenvironment. Springer, Dordrecht, pp. 293-328. https://doi.org/10.1007/978-90-481-9956-3_15

Kingston, J., Harrison, T., 2007. Isotopic dietary reconstructions of Pliocene herbivores at Laetoli: Implications for early hominin paleoecology. Palaeogeography, Palaeoclimatology, Palaeoecology 243, 272-306. https://doi.org/10.1016/j.palaeo.2006.08.002

Koenigswald, W. von., 2016. The diversity of mastication processes in Neogene and Quaternary proboscideans. Palaeontographica Abt. A 307, 1-41. https://doi.org/10.1127/pala/307/2016/1

Larramendi, A., 2016. Shoulder height, body mass and shape of proboscideans. Acta Palaeontologica Polonica 61, 537-574. https://doi.org/10.4202/app.00136.2014

Larramendi, A., Zhang, H., Palombo, M. R., Ferretti, M. P., 2020. The evolution of *Palaeoloxodon* skull structure: Disentangling phylogenetic, sexually dimorphic, ontogenetic, and allometric morphological signals. Quaternary Science Reviews 229, 106090. https://doi.org/10.1016/j.quascirev.2019.106090

Laws, R. M., 1966. Age criteria for the African elephant, *Loxodonta a. africana*. East African Wildlife Journal 4, 1-37. https://doi.org/10.1111/j.1365-2028.1966.tb00878.x

Leakey, M. G., Harris, J. M., 2003. Lothagam: Its significance and contributions. In: Leakey, M. G., Harris, J. M. (Eds.), Lothagam: The Dawn of Humanity in Eastern Africa. Columbia University Press, New York, pp. 625-655. https://doi.org/10.7312/leak11870-025

Leakey, M. G., Feibel, C. S., McDougall, I., Walker, A., 1995. New four-million-year-old hominid species from Kanapoi and Allia Bay, Kenya. Nature 376, 565-571. https://doi.org/10.1038/376565a0

Lee, P. C., Sayialel, S., Lindsay, W. K., Moss, C. J., 2011. African elephant age determination from teeth: Validation from known individuals. African Journal of Ecology 50, 9-20. https://doi.org/10.1111/j.1365-2028.2011.01286.x

Levin, N. E., Brown, F. H., Behrensmeyer, A. K., Bobe, R., Cerling, T. E., 2011. Paleosol carbonates from the Omo Group: Isotopic records of local and regional environmental change in East Africa. Palaeogeography, Palaeoclimatology, Palaeoecology 307, 75-89. https://doi.org/10.1016/j.palaeo.2011.04.026

Levin, N. E., Simpson, S. W., Quade, J., Cerling, T. E., Frost, S. R., 2008. Herbivore enamel carbon isotopic composition and the environmental context of *Ardipithecus* at Gona, Ethiopia. Geological Society of America Special Paper 446, 215-234. https://doi.org/10.1130/2008.2446(10)

Linneaus, C., 1758. Systema naturae per regna tria naturae, secundum classes, ordines, genera, species cum caracteribus, differentiis, synonymis, locis [System of nature, through the three kingdoms of nature, according to classes, orders, genera and species with characters, differences, synonyms and places]. Editio decima, reformata, Vol. 1. Holmiae: Laurentii Salvii. https://doi.org/10.5962/bhl.title.542

Lister, A. M., 2013. The role of behaviour in adaptive morphological evolution of African proboscideans. Nature 500, 331-334. https://doi.org/10.1038/nature12275

Lister, A. M., Sher, A. V., van Essen, H., Wei, G., 2005. The pattern and process of mammoth evolution in Eurasia. Quaternary International 126-128, 49-64. https://doi.org/10.1016/j.quaint.2004.04.014

MacInnes, D. G., 1942. Miocene and post-Miocene Proboscidia [sic] from East Africa. Transactions of the Zoological Society, London 25, 33-106. https://doi.org/10.1111/j.1096-3642.1942.tb00215.x

Mackaye, H. T., 2001. Les Proboscidiens du Mio-Pliocène du Tchad: Biodiversité, Biochronologie, Paléoécologie et Paléobiogeographie. Doctoral Dissertation, Université de Poitiers.

Mackaye, H. T., Brunet, M., Tassy, P., 2005. *Selenetherium kolleensis* gen. nov. sp. nov.: un nouveau Proboscidea (Mammalia) dans le Pliocène tchadien. Geobios 38, 765-777. https://doi.org/10.1016/j.geobios.2003.09.010

Mackaye, H. T., Coppens, Y., Vignaud, P., Lihoreau, F., Brunet, M., 2008. De nouveaux restes de *Primelephas* dans le Mio-Pliocène du Nord du Tchad et révision du genre *Primelephas*. Compte Rendus Palevol 7, 227-236. https://doi.org/10.1016/j.crpv.2008.03.007

Maglio, V. J., 1970. Four new species of Elephantidae from the Plio-Pleistocene of northwestern Kenya. Breviora 341, 1-43.

Maglio, V.J., 1971. Vertebrate faunas from the Kubi Algi, Koobi Fora and Ileret areas, East Rudolf, Kenya. Nature 231, 248-249. https://doi.org/10.1038/231248a0

Maglio, V. J., 1972. Evolution of mastication in the Elephantidae. Evolution 26, 638-658. https://doi.org/10.1111/j.1558-5646.1972.tb01970.x

Maglio, V. J., 1973. Origin and evolution of the Elephantidae. Transactions of the American Philosophical Society 63, 1-149. https://doi.org/10.2307/1006229

Maglio, V. J., Hendey, Q. B., 1970. New evidence relating to the supposed stegolophodont ancestry of the Elephantidae. South African Archaeological Bulletin 25, 85-87. https://doi.org/10.2307/3888130

Maglio, V. J., Ricca, A. B., 1977. Dental and skeletal morphology of the earliest elephants. Verhandelingen der Koninklijke Nedelandse Akademie van Wetenschappen, Afd., Natuurkunde Eerste Reeks, Deel 29, 1-51.

Manthi, F. K., Cerling, T. E., Chritz, K. L., 2017. Diets of mammalian fossil fauna from Kanapoi, northwestern Kenya. Journal of Human Evolution 140, 102338. https://doi.org/10.1016/j.jhevol.2017.05.005

Markov, G. N., 2008. The Turolian proboscideans (Mammalia) of Europe: Preliminary observations. Historia naturalis bulgarica 19, 153-178.

Mebrate, A., 1983. Late Miocene-Middle Pleistocene Proboscidean Fossil Remains from the Middle Awash Valley, Afar Depression, Ethiopia. Master's Thesis, University of Kansas.

Meyer, M., Palkopoulou, E., Baleka, S., Stiller, M., Penkman, K. E. J., Alt, K. W., Ishida, Y., Mania, D., Malickm, S., Meijer, T., Meller, H., Nagel, S., Nickel, B., Ostritz, S., Rohland, N., Schauer, K., Schüler, T., Roca, A. L., Reich, D., Shapiro, B., Hofreiter, M., 2017. Palaeogenomes of Eurasian straight-tusked elephants challenge the current view of elephant evolution. eLife 6: e25413. https://doi.org/10.7554/eLife.25413

McDougall, I., Brown, F. H., 2008. Geochronology of the pre-KBS Tuff sequence, Omo Group, Turkana Basin. Journal of the Geological Society, London 165, 549-562. https://doi.org/10.1144/0016-76492006-170

McDougall, I., Feibel, C. S., 1999. Numerical age control for the Miocene-Pliocene succession at Lothagam, a hominoid-bearing sequence in the northern Kenya Rift. Journal of the Geological Society, London 156, 731-745. https://doi.org/10.1144/gsjgs.156.4.0731

McDougall, I., Feibel, C. S., 2003. Numerical age control for the Miocene-Pliocene succession at Lothagam, a hominoid-bearing sequence in the northern Kenya Rift. In: Leakey, M. G., Harris, J. M. (Eds.), Lothagam: The Dawn of Humanity in Eastern Africa. Columbia University Press, New York, pp. 43-64. https://doi.org/10.7312/leak11870-004

McDougall, I., Brown, F. H., Vasconcelos, P. M., Cohen, B. E., Thiede, D. S., Buchanan, M. J., 2011. New single crystal ^{40}Ar/^{39}Ar ages improve time scale for deposition of the Omo Group, Omo-Turkana Basin, East Africa. Journal of the Geological Society, London 169, 213-226. https://doi.org/10.1144/0016-76492010-188

Patterson, B., Behrensmeyer, A. K., Sill, W. D., 1970. Geology and fauna of a new Pliocene locality in northwestern Kenya. Nature 226, 918-921. https://doi.org/10.1038/226918a0

Petrocchi, C., 1943. Il giacimento fossilero di Sahabi. Collezione Scientifica e Documentaria a Cura del Ministero dell'Africa Italiana, Verbania 12, 1-169.

Petrocchi, C., 1954. Paleontologia di Sahabi: Parte I. Proboscidati di Sahabi. Rendiconti Accademia nazionale dei XL 4-5, 8-74.

Pickford, M., Senut, B., Hadoto, D., 1993. Geology and Palaeobiology of the Albertine Rift Valley, Uganda-Zaire. Volume I: Geology. Occasional Publication 24, Centre International pour la Formation et les Echanges Géologiques, Orleans (France).

Roche, D., Ségalen, L., Senut, B., Pickford, M., 2013. Stable isotope analyses of tooth enamel carbonate of large herbivores from the Tugen Hills deposits: palaeoenvironmental context of the earliest Kenyan hominids. Earth and Planetary Science Letters 381, 39-51. https://doi.org/10.1016/j.epsl.2013.08.021

Roth, V. L., 1989. Fabricational noise in elephant dentitions. Paleobiology 15, 165-179. https://doi.org/10.1017/S0094837300009349

Saarinen, J., 2019. The palaeontology of browsing and grazing. In: Gordon, I. J., and Prins, H. H. T. (Eds.), The Ecology of Browsing and Grazing II. Ecological Studies 239, Springer Nature, Switzerland, pp. 5-59. https://doi.org/10.1007/978-3-030-25865-8_2

Saegusa, H., 2020. Stegodontidae and *Anancus*: Keys to understanding dental evolution in Elephantidae. Quaternary Science Reviews 231, 106176. https://doi.org/10.1016/j.quascirev.2020.106176

Saegusa, H., Haile-Selassie, Y., 2009. Proboscidea. In: Haile-Selassie, Y., WoldeGabriel, G. (Eds.), *Ardipithecus Kadabba*. Late Miocene Evidence from the Middle Awash, Ethiopia. University of California Press, Berkeley, pp. 469-516. https://doi.org/10.1525/california/9780520254404.003.0015

Sanders, W. J., 1990. Fossil Proboscidea from the Pliocene Lusso Beds of the Western Rift, Zaire. In: Boaz, N. T. (Ed.), Evolution of Environments and Hominidae in the African Western Rift Valley. Virginia Museum of Natural History Memoir No. 1, Martinsville, Virginia, pp. 171-187.

Sanders, W. J., 1997. Fossil Proboscidea from the Wembere-Manonga Formation, Manonga Valley, Tanzania. In: Harrison, T. (Ed.), Neogene Paleontology of the Manonga Valley, Tanzania. Plenum Press, New York, pp. 265-310. https://doi.org/10.1007/978-1-4757-2683-1_9

Sanders, W. J., 2007. Taxonomic review of fossil Proboscidea (Mammalia) from Langebaanweg, South Africa. Transactions of the Royal Society of South Africa 62, 1-16. https://doi.

org/10.1080/00359190709519192

Sanders, W. J., 2008. Review of fossil Proboscidea from the late Miocene-early Pliocene site of As Sahabi, Libya. Garyounis Scientific Bulletin Special Issue No. 5, 217-239.

Sanders, W. J., 2011. Proboscidea. In: Harrison, T. (Ed.), Paleontology and Geology of Laetoli: Human Evolution in Context. Volume 2: Fossil Hominins and the Associated Fauna. Springer, New York, pp. 233-262. https://doi.org/10.1007/978-90-481-9962-4_9

Sanders, W. J., 2017. Horizontal tooth displacement and premolar occurrence in elephants and other elephantiform proboscideans. Historical Biology 30, 137-156. https://doi.org/10.1080/08912963.2017.1297436

Sanders, W. J., 2020. Proboscidea from Kanapoi, Kenya. Journal of Human Evolution 140, 102547. https://doi.org/10.1016/j.jhevol.2018.10.013

Sanders, W. J., In press. Proboscidea. In: Bibi, F., Kratz, B., Beech, M., Hill, A. (Eds.), Sands of Time: Late Miocene Fossils from the Baynunah Formation, U.A.E. Springer, Cham, Switzerland.

Sanders, W. J., Haile-Selassie, Y., 2012. A new assemblage of mid-Pliocene proboscideans from the Woranso-Mille Area, Afar Region, Ethiopia: Taxonomic, evolutionary, and paleoecological considerations. Journal of Mammalian Evolution 19, 105-128. https://doi.org/10.1007/s10914-011-9181-y

Sanders, W. J., Gheerbrant, E., Harris, J. M., Saegusa, H., Delmer, C., 2010. Proboscidea. In: Werdelin, L., Sanders, W. J. (Eds.), Cenozoic Mammals of Africa. University of California Press, Berkeley, pp. 161-251. https://doi.org/10.1525/california/9780520257214.003.0015

Schoeninger, M. J., H. Reeser, H., Hallin, K., 2003. Paleoenvironment of *Australopithecus anamensis* at Allia Bay, East Turkana, Kenya: Evidence from mammalian herbivore enamel stable isotopes. Journal of Anthropological Archaeology 22, 200-207. https://doi.org/10.1016/S0278-4165(03)00034-5

Schuster, M., Duringer, P., Ghienne, J.-F., Roquin, C., Sepulchre, P., A. Moussa, A., Lebatard, A.-E., Mackaye, H. T., Likius, A., Vignaud, P., Brunet, M., 2009. Chad Basin: Paleoenvironments of the Sahara since the late Miocene. Compte Rendus Geoscience 341, 603-611. https://doi.org/10.1016/j.crte.2009.04.001

Strömberg, C. A. E., 2011. Evolution of grasses and grassland ecosystems. Annual Review Earth and Planetary Sciences 39, 517-544. https://doi.org/10.1146/annurev-earth-040809-152402

Tassy, P., 1983. Les Elephantoidea miocènes du Plateau du Potwar, Groupe de Siwalik, Pakistan. II^e Partie : choerolophodonts et gomphothères. Annales de Paléontologie 69, 235-298.

Tassy, P., 1985. La place des mastodontes miocènes de l'ancien monde dans la phylogénie des Proboscidea (Mammalia) : Hypothèses et conjectures. PhD Dissertation, Université Pierre et Marie Curie, Paris.

Tassy, P., 1995. Les Proboscidiens (Mammalia) Fossiles du Rift Occidental, Ouganda. In: Pickford, M., Senut, B. (Eds.), Geology and Palaeobiology of the Albertine Rift Valley, Uganda-Zaire. Vol. II: Palaeobiology. CIFEG Occasional Publications, 1994/29, Orléans, pp. 217-257.

Tassy, P., 1999. Miocene elephantids (Mammalia) from the Emirate of Abu Dhabi, United Arab Emirates: Palaeobiogeographic implications. In: Whybrow, P. J., Hill, A. (Eds.), Fossil Vertebrates of Arabia. With Emphasis on the late Miocene Faunas, Geology, and Palaeoenvironments of the Emirate of Abu Dhabi, United Arab Emirates. Yale University Press, New Haven, pp. 209-233.

Tassy, P., 2003. Elephantoidea from Lothagam. In: Leakey, M. G., Harris, J. M. (Eds.), Lothagam: The Dawn of Humanity in Eastern Africa. Columbia University Press, New York, pp. 331-358. https://doi.org/10.7312/leak11870-014

Tassy, P., 2013. L'anatomie cranio-mandibulaire de *Gomphotherium angustidens* (Cuvier, 1817) (Proboscidea, Mammalia): données issues du gisement d'En Péjouan (Miocène moyen du Gers, France). Geodiversitas 35, 377-445. https://doi.org/10.5252/g2013n2a6

Todd, N. E., 2010. Qualitative comparison of the cranio-dental osteology of the extant elephants, *Elephas maximus* (Asian elephant) and *Loxodonta africana* (African elephant). The Anatomical Record 293, 62-73. https://doi.org/10.1002/ar.21011

Uno, K. T., Cerling, T. E., Harris, J. M., Kunimatsu, Y., Leakey, , M. G., Nakatsukasa, N., Nakaya, N., 2011. Late Miocene to Pliocene carbon isotope record of differential diet change among East African herbivores. Proceedings of the National Academy of Sciences, USA 108, 6509-6514. https://doi.org/10.1073/pnas.1018435108

Van der Merwe, N. J., Bezuidenhout, A. J., Seegers, C. D., 1995. The skull and mandible of the African elephant (*Loxodonta africana*). Onderstepoort Journal of Veterinary Research 62, 245-260.

Wang, S.-Q., Saegusa, H., Duangkrayom, J., He, W., Chen, S.-Q., 2017. A new species of *Tetralophodon* from the Linxia Basin and the biostratigraphic significance of tetralophodont gomphotheres from the Upper Miocene of northern China. Palaeoworld 26, 703-717. https://doi.org/10.1016/j.palwor.2017.03.005

Warny, S. A., Bart, P. J., Suc, J.-P., 2003. Timing and progression of climatic, tectonic and glacioeustatic influences on the Messinian Salinity Crisis. Palaeogeography, Palaeoclimatology, Palaeoecology 202, 59-66. https://doi.org/10.1016/S0031-0182(03)00615-1

White, T. D., Moore, R. V., Suwa, G., 1984. Hadar biostratigraphy and hominid evolution. Journal of Vertebrate Paleontology 4, 575-583. https://doi.org/10.1080/02724634.1984.10012033

Zazzo, A., Bocherens, H., Brunet, M., Beauvilain, A., Billiou, D., Mackaye, H. T., Vignaud, P., Mariotti, A., 2000. Herbivore paleodiet and paleoenvironmental changes in Chad during the Pliocene using stable isotope ratios of tooth enamel carbonate. Paleobiology 26, 294-309. https://doi.org/10.1666/0094-8373(2000)026<0294:HPAPCI>2.0.CO;2

Zhang, H., 2020. Evolution and Systematics of the Elephantidae (Mammalia, Proboscidea) from the Late Miocene to Recent. Doctoral Dissertation, University of Bristol School of Earth Sciences.

Zhang, H., Pape, T., Lister, A.M., 2018. On the type material of *Elephas hysudrindicus* Dubois, 1908 (Mammalia, Proboscidea). Journal of Vertebrate Paleontology 28,1, e1425211. https://doi.org/10.1080/02724634.2017.1425211